NASA CR-72035
TR 467-Final

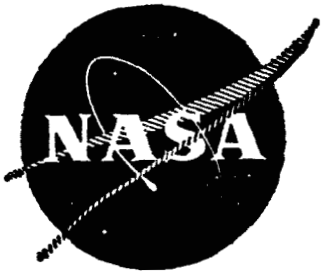

CAVITATION DAMAGE IN LIQUID METALS

by

A. Thiruvengadam and H. S. Preiser

prepared for

NATIONAL AERONAUTICS AND SPACE ADMINISTRATION

CONTRACT NAS 3-4172

NOVEMBER 1965

HYDRONAUTICS, incorporated
research in hydrodynamics

Research, consulting, and advanced engineering in the fields of NAVAL and INDUSTRIAL HYDRODYNAMICS. Offices and Laboratory in the Washington, D. C., area: Pindell School Road, Howard County, Laurel, Md.

(over)

NOTICE

This report was prepared as an account of Government sponsored work. Neither the United States, nor the National Aeronautics and Space Administration (NASA), nor any person acting on behalf of NASA:

(a) Makes any warranty or representation, expressed or implied, with respect to the accuracy, completeness, or usefulness of the information contained in this report, or that the use of any information, apparatus, method, or process disclosed in this report may not infringe privately owned rights; or

(b) Assumes any liabilities with respect to the use of, or for damages resulting from the use of any information, apparatus, method or process disclosed in this report.

As used above,"person acting on behalf of NASA" includes any employee or contractor of NASA, or employee of such contractor, to the extent that such employee or contractor of NASA, or employee of such contractor prepares, disseminates, or provides access to, any information pursuant to his employment or contract with NASA, or his employment with such contractor.

Requests for copies of this report should be referred to:

National Aeronautics and Space Administration
Office of Scientific and Technical Information
Post Office Box 33
College Park, Maryland 20740

HYDRONAUTICS, Incorporated

NASA CR-72035
TR 467 - Final

Final Report

CAVITATION DAMAGE IN LIQUID METALS

By

A. Thiruvengadam and H. S. Preiser

Prepared for

National Aeronautics and Space Administration
Contract NAS 3-4172
November 29, 1965

Technical Management
NASA Lewis Research Center
Cleveland, Ohio
Nuclear Power Technology Branch
James P. Couch

HYDRONAUTICS, Incorporated
Pindell School Road
Laurel, Maryland

TABLE OF CONTENTS

I. ABSTRACT

This is the final report summarizing the results of investigations on the cavitation damage resistance, the high frequency fatigue and the stress corrosion behavior of five metals in liquid sodium up to 1500°F. The test duration is an important parameter in evaluating the relative cavitation damage resistance. Stellite 6B exhibits the greatest resistance as compared with Cb-132M, T-222, TZM and 316 stainless steel. The rate of damage decreases with increasing temperature.

High frequency fatigue tests at ~35 ppm and at ~100 ppm oxide contamination in liquid sodium up to 1500°F show that the oxide content does not change the fatigue behavior of TZM and 316 stainless steel. The fatigue of 316 stainless steel in 1500°F sodium at 14,000 cps is comparable with the results obtained at 1500°F vacuum (3×10^{-5} torr) at 4-5 cps. No stress corrosion cracking was observed on TZM and on 316 stainless steel over a 60 hour test at two oxide levels (~35 ppm and ~100 ppm) in liquid sodium at two temperatures (1000°F and 1500°F) up to 100 percent yield.

II. INTRODUCTION

High output Rankine-cycle space power systems, using nuclear reactors as their prime energy sources, will use alkali metals as their heat transfer and working fluids operating at temperatures up to 2200°F. These power systems must perform reliably for long periods (perhaps one to three years) of unattended service. Cavitation of the working fluid in these systems is possible because liquid condensate will be transferred under transient conditions favorable to the formation of vapor bubbles. The formation and growth of these vapor bubbles during cavitation and their ultimate collapse on metal surfaces at local areas of higher pressure in pumps, piping and other critical components of the system can cause extensive damage. Therefore, materials must be found to resist this cavitation damage or design conditions must be controlled to prevent the occurrence of cavitation.

Two recent studies have shown that cavitation damage can be a limiting factor of design for long duration operation of a space system. In one study, Smith, DeVan and Grindell (Reference 1) reported an erosion depth of 0.34 inch in an Inconel impeller pumping liquid sodium in a temperature range of 1050°F-1250°F for a period of 2575 hours. In the other study, an endurance test specifically designed for obtaining some knowledge of the intensity of damage on a 316 stainless steel impeller pumping potassium at a constant temperature of 1400°F, showed erosion depths up to 0.05 inch in 350 hours of operation (Reference 2). This pump was operating at a speed of 6375 rpm and

delivering 710 gpm against 200 feet of head. It seems clear that cavitation damage could be a serious problem if the operating period of these tests were increased to, say, 10,000 hours coupled with the criteria of light weight and superior reliability.

These considerations motivated the National Aeronautics and Space Administration to sponsor a broad based basic investigation on the mechanism of cavitation damage in liquid metals at high temperatures. To study this phenomenon, an experimental apparatus was developed making use of the magnetostriction transducer generally used for such studies in water at room temperature (Reference 3). Using the experience gained in earlier experiments, a new facility was developed for conducting cavitation damage studies on refractory metals (References 3 and 4). This facility is capable of maintaining liquid sodium at temperatures up to 1500°F with oxygen impurity levels of less than 30 ppm over an operating time of 8 hours (Reference 5).

With the aid of this new facility, basic information was obtained on several aspects of the mechanism of cavitation damage, particularly the effect of temperature on the intensity of cavitation damage (Reference 6). Several metals were tested for their cavitation damage resistance including three refractory alloys; Cb-132M, T-222, and TZM at 400°F, 1000°F and 1500°F (Reference 7). New techniques were developed under this program for testing high frequency fatigue and stress corrosion cracking of high temperature alloys to determine if these parameters were significant in explaining the response of materials to cavitation attack.

III. EXPERIMENTAL FACILITIES AND TECHNIQUES

1. Experimental Facilities

The operational experience gained on an earlier experimental facility is described in Reference 3. These experiences led to the design of a more sophisticated apparatus currently in use. Since the details of the design as well as the calibration of this facility are described in Reference 5, only a brief outline of its features and capabilities are presented in this report.

The experimental facility consists essentially of the following systems: (Figure 1)

1. Controlled Environment Dry Box
2. Cover Gas Systems
3. Liquid Metal System
4. Heating and Cooling Systems
5. Magnetostriction Apparatus

Controlled Environment Dry Box

This is a 304 stainless steel chamber designed to be evacuated to a minimum pressure of 2.5 millitorr prior to back flushing with pure argon cover gas. A standard sloped-front dry box was modified with special access openings for an air lock, heated specimen lock, tubular housing for the magnetostriction device, rear door, view ports, lighting ports, utilities and instrument connections. A false bottom is fabricated in the box for cooling purposes. The general arrangement is

shown in Figure 1. A 15 cfm mechanical vacuum pump can evacuate air from this dry box down to 2.5 millitorr in 8 hours with an in leak rate of less than 15 millitorr per hour. The retort, air lock and specimen lock can be evacuated rapidly and separately, independent of the main chamber to a vacuum of 2.5 millitorr also.

Cover Gas System

An inert atmosphere of pure argon surrounds all components which are in contact with or have access to the liquid sodium. Commercially available, high purity argon, with total moisture, oxygen and nitrogen of less than 5 ppm, is used to fill the dry box, retort, air lock and specimen lock after evacuation. The oxygen and moisture levels in the argon are monitored at discharge from the storage flasks, in the manifold, and in the dry box.

The cover gas system is capable of introducing an initial charge of argon (PVC glove ports closed) containing one ppm each of O_2 and H_2O. During a typical experimental run the argon atmosphere in the dry box contaminates at 8 ppm/hr for H_2O with the glove ports open. However, during an experiment the argon cover gas in the retort is not in contact with the atmosphere in the dry box proper, except for very short intervals during specimen removal for weighing, and therefore the retort atmosphere over the sodium is probably of much higher purity.

Liquid Metal System

This system consists of a storage tank, hot trap, retort and dump tank. For the present studies, commercially pure, reactor grade liquid sodium was procured in 30 gallon reinforced stainless steel drums. The sodium from this drum was heated to 500°F and transferred to the hot trap by means of pressure from the high purity argon supply.

To further purify the reactor grade sodium to 10 ± 10 ppm oxide content, it was hot-trapped with zirconium chips for 72 hours at 1400°F. This sodium was again pumped by argon displacement into a retort which is located in the bottom of the dry box. This retort is made of a high nickel alloy and is bolted to the floor of the dry box through a high temperature, vacuum tight flanged joint. The retort can withstand up to 5 psig pressure at 1500°F. After the experiment, the sodium can be drained from the retort to a dump tank. The entire sodium transfer loop is made of 316 stainless steel tubing and fitted with bellows-sealed, vacuum-tight, control valves.

Heating and Cooling Systems

The components associated with the heating system are the retort furnace, hot-trap furnace, vacuum furnace, storage and dump tank heaters and traced line heaters for sodium transfer pipes.

The floor of the dry box is maintained at 70°F at a 12 inch radius from the center of the retort. The maximum temperature of the retort head does not exceed 400°F, and the argon

temperature inside the box does not rise above 90°F while the retort is operated at 1500°F. The magnetostriction transducer is cooled to room temperature by a constant temperature kerosene bath.

Magnetostriction Apparatus

The magnetostriction apparatus vibrates a test specimen rapidly in the hot liquid metal to form cavitation bubbles during the up-stroke which collapse on the specimen during the down-stroke to produce the desired damage. This repetitive cycle leads to measurable damage rates under carefully controlled laboratory conditions.

The magnetostriction apparatus consists of a nickel transducer and velocity transformer, which is caused to oscillate in a resonant condition by an alternating magnetic field furnished from a sine generating power supply as shown in Figure 2. The apparatus was housed in a suitable elevating mechanism to permit operation in the dry box. Special precautions had to be taken to design a pick-up coil (for monitoring the amplitude of vibration) which would be shielded from the hot sodium vapor in the retort. A feedback control circuit was also incorporated in system electronics which provided continuous stable frequency and amplitude output of the apparatus despite local fluctuations in operating temperature gradients. The details of design have been described in References 3 - 8.

2. Experimental Techniques

Cavitation Damage Resistance Tests

Reference 9 presents a detailed study of the effect of various test parameters on the cavitation damage produced by a magnetostriction device. The reproducibility of results with a simple flat faced test specimen is equivalent to other more complex specimen shapes. The dimensions of the liquid container within wide limits have a relatively insignificant effect on the test results. The same conclusion holds good for the depth of immersion of the specimen in the test liquid. The rate of volume loss varies as the square of specimen diameter in the steady state zone.

Based on these observations, the following test parameters used in this program were selected: A simple flat faced specimen of half an inch radius was vibrated at a double amplitude of 1.36×10^{-3} inch and a frequency of 14 kcs to obtain the relationship between the damage rate and the test duration until the steady state zone was reached.

High Frequency Fatigue Tests

A high frequency fatigue test, using a modified magnetostriction apparatus, was devised to assess the significance of strain rate and corrosion effects on correlating material parameters affecting cavitation damage rates. The frequency of loading and the liquid metal environment were controlled to duplicate experimental conditions of the cavitation damage tests.

Some earlier investigations describing the technique of high frequency fatigue at room temperature are cited for background information (References 10, 11, 12 and 13).

The basic principle of the design of the high frequency fatigue specimens is as follows: When a longitudinal vibration of a half wave length of a metallic rod is produced by means of an oscillator, the maximum strain is produced at the node while the maximum velocity and displacement are produced at the antinodes at either end of the rod (Figure 3). If a notch is produced at the node, then the strain is further amplified at the node. It is necessary to amplify the strains by means of a notch because of the power limitations of the driving oscillator. However, there are two undesirable side effects due to this notch, namely: (i) the fatigue notch sensitivity and (ii) the change in resonant frequency which will be discussed subsequently.

A half wave length of the metallic rod is attached to the free end of the velocity transformer and it is vibrated at the most efficient operating frequency of the magnetostriction device. The half wave length can be experimentally determined by adjusting the rod length to resonate at the operating frequency. An accurate determination of this length and frequency will give the value of velocity of sound for each of the metals tested by the relationship:

$$\lambda f_n = c \qquad [1]$$

where

λ is the wave length,

f_n is the resonant frequency, and

c is the velocity of sound.

The modulus of elasticity for each metal can be calculated after determining the density of each metal, by:

$$E = \rho c^2 \qquad [2]$$

where

E is the modulus of elasticity, and

ρ is the density of the metal.

Table 1 gives the physical properties thus determined for each of the two metals tested at two temperatures.

Notch sensitivity - A notch was provided at the node to produce high strains in the test material. It is known that fatigue strength is sensitive to notches and is dependent upon the geometry of the notch. This notch effect on fatigue strength is characterized by a factor η, known as notch sensitivity and is given by:

$$\eta = \frac{K_f - 1}{K_t - 1} \qquad [3]$$

where

$$K_f = \frac{\text{un-notched fatigue strength}}{\text{notched fatigue strength}}, \text{ and}$$

K_t = the theoretical stress concentration factor.

Experimental information on η as a function of notch radius at elevated temperatures is not readily available. The notch radius for room temperature studies was selected so that η would be as close to unity as possible (Reference 14). The same notch radius was adopted for high temperature studies also since no experimental data were readily available for the metals under test. The theoretical stress concentration factors for round bars can be found in Reference 14. The dimensions of the notch selected are shown in Figure 4.

The stresses are calculated as follows: The maximum strain at the node for a uniform rod in sinusoidal vibration is given by:

$$\epsilon_{max} = \frac{2\pi \xi_{max}}{\lambda} \qquad [4]$$

where ξ_{max} is the maximum amplitude. The stress amplitude σ_a is given by:

$$\sigma_a = \epsilon_{max} \cdot E \qquad [5]$$

For the present specimen design, the theoretical stress concentration factor taken from Reference 14 is 1.65. A magnification of the maximum strain will occur at the notched section equal to the stress concentration factor multiplied by the ratio of cross sectional areas of the unnotched and notched portions of the specimen, which is 1.65 x 4 or 6.6. Therefore, the stress amplitude of the notched specimen is given by:

$$\sigma_a = 6.6 \frac{2\pi}{\lambda} \xi_{max} \cdot E \qquad [6]$$

Effect of notch on resonant frequency - Another effect of the notch is to lower the resonant frequency slightly. This problem can be rectified by reducing the length of the fatigue specimen with a few trial and error experiments. This modified length can also be predicted by an approximate theory following Neppiras (Reference 11). However, the change in wave length due to the notch (twice the specimen length) remains within 10 percent of the unnotched wave length, λ, as shown in Table 1. This notched wave length should be used in the calculation of strains in Equation [4].

Stress Corrosion Tests

Under repetitive cavitation collapse forces, the test material can become severely worked and build up internal residual stresses. Therefore some limited stress corrosion tests on 316 stainless steel and TZM in high temperature liquid sodium were also conducted as part of this program to determine if this parameter was significant in fracturing the material.

There are two methods in normal use for producing stress corrosion cracking: constant strain and constant load. Under constant strain the specimen is loaded to a fixed value and upon cracking the stress is relieved, thereby tending to reduce the rate of cracking. In the constant load device, as cracking develops the stress is increased due to a decrease in cross-sectional area at the crack. At this point, the cracking rate is increased and therefore is readily identified.

The first method (constant strain) employs a typical horseshoe shaped specimen or bent beam in a fixed holder, while the second method generally employs a tensile type specimen loaded by weights. The susceptibility of a metal to stress corrosion cracking can be readily demonstrated by the first method, while a parametric study of the amount of stress versus time to fail is more easily obtained with a constant load apparatus.

A condition for the method selected was that it be easily adaptable for testing in the limited space available in the retort of the present facility. This consideration led to the selection of a split ring type of stress corrosion specimen (Figure 5) which is a modification of the horseshoe type. In this case a constant strain is produced by closing the gap of a split ring.

The relationship between the maximum deflection δ_v produced by a load P in a thin split ring of thickness, d and breadth, b (see Figure 5), is given by the following equation (Reference 15):

$$\delta_v = \frac{6\pi\ Pr^3}{E\ bd^3} \qquad [7]$$

where

E is the modulus of elasticity of the material, and

r is the radius of the thin ring.

Figure 6 shows good agreement between theory and actual measured values of load and deflection. A variable reluctance force gage was used in making the measurements. The maximum fiber stress, σ, corresponding to a deflection δ_v is given by:

$$\sigma = \frac{Ed\delta_v}{\pi r^2} \qquad [8]$$

By fabricating the entire specimen assembly from the same material, no additional stresses were introduced upon heating as all parts expand equally. The appropriate value of the Youngs modulus E for a given temperature was determined from the fatigue experiments.

IV. MATERIALS TESTED

The following materials were tested in this program for their cavitation damage resistance in liquid sodium:

a. 316 stainless steel

b. Stellite 6B (Cobalt alloy)

c. TZM (Titanium-Zirconium-Molybdenum alloy)

d. T-222 (Ta-10W-2.5 Hf alloy)

e. Cb-132M (Columbium-Tantalum-Tungsten-Molybdenum alloy)

(a) 316 stainless steel - An 18-8 chromium-nickel stainless steel, particularly suited for high temperature service. It is similar to type 304, except that the addition of molybdenum greatly increases its creep strength at elevated temperatures. It is useful in high strength service up to approximately 1500°F and resistant to oxidation up to 1650°F. The material cannot be hardened by heat treatment. The stock was delivered in the cold drawn, annealed condition from the manufacturer. The specimens were used for the tests in the "as received" condition, after machining without further annealing.

(b) Stellite 6B - A cobalt based alloy with a relatively moderate (1.1 percent) carbon content, making it one of the easiest of the cobalt based alloys to form and work. The bar stock was furnished in the hot rolled condition and no further heat treatment was provided after machining.

(c) TZM (Titanium-Zirconium-Molybdenum) - A 0.5 percent Ti, 0.1 percent Zr, Mo based alloy, similar to the more common Mo-0.5 Ti, but having greater hot strength and a higher recrystallization temperature. Elevated temperature strength is brought about by a combination of strain hardening and precipitation of complex carbides causing dispersion hardening. The TZM bar stock was furnished in the stress relieved condition by reheating above the recrystallization temperature to 2250°F for one-half hour. No further heat treatment was provided after machining.

(d) T-222 (Ta-10W-2.5 Hf) - This is a tantalum based alloy similar to T-111 (Ta-8W-2Hf) but it exhibits superior strength from approximately 2000°F to 3500°F. The alloy retains its ductility for easy forming and also has excellent corrosion resistance, probably due to the presence of hafnium carbides. The material was received from the manufacturer in the stress relieved and annealed condition by vacuum annealing in a tungsten element furnace for one hour at 2200°F. No further heat treatment was provided after machining the specimens.

(e) Cb-132M - This columbium based alloy is modified with reactive metals such as hafnium or zirconium to minimize alkali metal corrosion attack. This particular alloy was furnished along with preliminary information on its properties, by NASA. The fabrication history and heat treatment data were not available for the specimens tested.

Though all these five metals were tested for their cavitation damage resistance, only 316 stainless steel and TZM were selected for high frequency fatigue and stress corrosion tests at 1000°F and at 1500°F. Table 3 contains the nominal chemical compositions of the test metals used.

V. RESULTS AND ANALYSIS

1. Cavitation Damage Resistance Tests

Effect of Testing Time on the Rate of Cavitation Damage

Until recently it has been the general practice to test all materials over an arbitrarily selected constant duration, and to compare the cumulative damage as an indication of

the cavitation damage resistance. However, it is now known that the rate of damage is time dependent (References 16,9,17) and this relationship can be divided into four different zones of damage:

(a) Incubation zone - The incubation zone has been defined as the time during which "little" or no weight loss occurs.

(b) Accumulation zone - After incubation, the material starts absorbing more and more energy giving rise to increased fracture and weight loss.

(c) Attentuation zone - The rate of damage reaches a peak in the accumulation zone and then begins to decline. The beginning of this zone is characterized by isolated deep craters.

(d) Steady state zone - The zone in which the rate of weight loss reaches a constant value after declining in the attenuation zone. In this zone the cavitation damage rate is observed to be time independent and thus far it is in this zone that the most successful correlations of cavitation damage with material parameters have been made.

The existence of these zones have been confirmed for several metals and in various liquid environments (Reference 17).

To make a meaningful comparison of the performance of the five metals tested under this program, the relationship between the test duration and the rate of damage were obtained and are

shown in Figures 7 through 11 at 400°F. Each data point represents one measurement of weight loss. A summarized presentation in Figure 12 reveals the importance of knowing such relationships for these metals. While T-222 requires fourteen hours to reach steady state, TZM reaches that zone in only four hours. Although the steady state damage rates are comparable for 316 stainless steel and for TZM, the initial rates of damage for TZM are markedly higher.

The fact that the curves in Figure 12 cross each other indicates that each one of the five metals tested exhibits its own characteristic response. An explanation of these specific response characteristics in the first two zones is considered possible through better understanding of the behavior of these metals at high rates of straining at elevated temperatures and of the process of energy accumulation during repeated loading. An understanding of the third zone of damage, the attenuation zone (characterized by the formation of isolated deep craters) is related to the surface roughness of the material which in turn affects the hydrodynamics of bubble collapse (Reference 9). This view is supported by some recent experimental evidence indicating that artificial roughness simulating cavitation damage will eliminate or reduce the peak in the transition to the steady state zone (Reference 17). More detailed investigations are required to resolve these aspects of the damage rate behavior.

Relative Cavitation Damage Resistance of Refractory Alloys

In the steady state zone where damage rate is independent of testing time, the five metals tested at 400°F may be placed in the following order of merit starting from the best:

a. Stellite 6B
b. Cb-132M
c. T-222
d. TZM
e. 316 stainless steel

Figure 13 shows the cavitation damage resistance of the five alloys in sodium at 1000°F and at 1500°F. Figure 14 shows photographs of the cavitation damage pattern in the steady state zone* after exposure to 1500° sodium.

It should be noted that the experiments at 1000°F and at 1500°F were conducted with the same specimens that were used to obtain the steady state zone at 400°F sodium. This procedure was adopted because the relatively lower rates of damage observed at higher temperature (as discussed subsequently in this report) would require inordinately long testing periods to achieve damage in the steady state zone. Some initial experiments reported in Reference 5 showed that only surface indentations could be observed on 316 stainless steel at 1000°F even after 25 hours of testing. However, the use of specimens prepared in the steady state zone at another temperature was

* Stellite 6B did not reach the steady state zone.

considered valid in view of the fact that previous data had shown that specimens prepared in the steady zone at one intensity (amplitude) continued to damage at a constant but different rate at another temperature (9).

Effect of Estimated Strain Energy

There have been many attempts in the past to correlate the mechanical properties of the test material with cavitation damage. One can get a clear picture of the controversies existing in this area from the review articles in the technical literature (e.g., Reference 18). Recent efforts to correlate cavitation damage resistance with the strain energy of the material (area of the engineering stress-strain diagram from a simple tensile test) have offered some promise (References 19,20). From the beginning, these efforts have been handicapped by the lack of actual stress-strain information even for tests at room temperature. At higher temperatures, the attempts to obtain actual strain energies become much more difficult. However, the typical values of ultimate tensile strength, yield strength and ultimate elongation can be obtained from published literature as a function of temperature and can be used to estimate the magnitude of strain energy by the use of the following approximate relationship (Reference 20):

$$S_e = \frac{(Y + T)}{2} \epsilon \qquad [9]$$

where

Y is the yield strength,

T is the ultimate tensile strength, and

ϵ is the ultimate elongation.

Such estimated values of strain energy were used in an earlier investigation, wherein the oxide level of the liquid sodium was believed to be near saturation at 400°F. The correlation obtained at 400°F is shown in Figure 15 (Reference 21). Similar estimates of strain energy as a function of temperature were made for the five alloys tested under this program and are shown in Figure 16* (Reference 5). The relationship between the estimated strain energy and the reciprocal of rate of volume loss at 1000°F is shown in Figure 17.

The data for Stellite 6B is not plotted in Figure 17 since it was not tested in the steady state zone. Considering the fact that the values of mechanical properties are only typical values reported in the literature and that they may vary from heat to heat and thermal treatments**, the results in Figure 17 generally confirm the earlier findings that the energy absorption characteristics of metals during fracture represent their cavitation damage resistance.

---

* Cb-132M data are not available for publication.

** In fact the strain energy of TZM as estimated was based on the short time tensile strength of the recrystallized material. The short time tensile strength of stress-relieved, as-rolled TZM is 30 percent lower than that of the recrystallized form.

Recent experiments by Young and Johnston (22) also confirm the correlation between cavitation damage resistance and the strain energy of the material estimated approximately by Equation [9]. However, they underrate the significance of strain energy because data on Stellite 6B does not fit into this correlation. However, the apparent anomalous behavior of Stellite can be explained by considering the following facts.

1. Stellite 6B has not reached the steady state in either experiment, and therefore the rate of damage could be much higher in the steady state.

2. The weight loss measurements of the order of 0.1 milligrams in a typical 30 minute test run on Stellite are unreliable at the intensity of damage obtained with a magnetostriction device. In our experiments, it was sometimes noticed that an increase in weight of the specimen occurred, presumably due to moisture accumulation during weighing.

3. The estimated strain energy value may be much lower than the actual area of the stress-strain diagram. This is because Equation [9] assumes the stress-strain diagram to be a trapezium whereas the actual shape could be considerably different depending upon the material and temperature of the test.

In spite of the above discrepancy of Stellite, the data of Young and Johnston in general shows a good correlation with strain energy, and the significance and usefulness of this correlating parameter should not be overlooked. Much more detailed and intensive investigations are necessary for

confirming these relatively limited results. The need for reliable mechanical properties at these temperatures and at these high strain rates is of paramount importance.

Intensity of Cavitation Damage

One of the useful results of this correlation is the justification for the use of the strain energy (as estimated in this report) in calculating the intensity of cavitation damage. This intensity has been defined as the power absorbed per unit area of the material (Reference 16) and is given by

$$I = \frac{iS_e}{t} \qquad [10]$$

where

I is the intensity of cavitation damage,

i is the average depth of erosion,

S_e is the strain energy of the material, and

t is the duration of erosion.

The estimation of this intensity parameter would be particularly useful for the case of full scale machines such as liquid metal pumps since any operating experience can be analyzed in a quantitative manner. A nomogram, called cavitation damage intensity estimator, has been prepared using Equation [10] for use in low temperature liquids such as water (Reference 23). A similar nomogram may be useful for high temperature liquid metals as well, once the validity of the strain energy correlation is proved.

Effect of Liquid Sodium Temperature on Cavitation Damage

One of the basic parameters in the study of cavitation damage in liquid metals is the temperature of the liquid metal. Using a 316 stainless steel specimen that had reached the steady state at one temperature, a series of experiments were conducted in the dry box over a range of temperatures between 300°F to 1500°F, at 100°F intervals, in order to determine the variation of the rate of cavitation damage with the temperature of the sodium (Reference 6). The duration of each experiment was one hour and the results of these experiments are shown in Fiugre 18. The rate of weight loss at 1500°F is of the order of a hundredth of a milligram per hour as compared to 16 mg/hour at 400°F.

A minimum of three readings were taken at each temperature in order to check the reproducibility of the data. The precautions for obtaining high purity sodium were observed throughout these experiments.

The intensity of cavitation damage was computed using the weight loss data shown in Figure 18 and the estimated strain energy values discussed earlier (See also Table 2). Figure 19 shows the effect of temperature of liquid sodium on the intensity of cavitation damage. To obtain a relative idea of the order of magnitude of the decrease in intensity at higher temperatures, the relative intensity with respect to the intensity at 400°F is plotted in Figure 20 as a function of temperature.

The effect of liquid temperature on cavitation damage has been the subject of investigations since 1937 (24). The relative role of the liquid properties that give rise to the increase in damage with temperature near the melting point of liquid and to the decrease in damage with increasing temperature near about the boiling point of the liquid has been a subject of speculation since that time. It is also not clear why there is so much difference in damage rates from liquid to liquid, particularly the damage rates in hydrocarbon liquids, which are about a tenth of that in water. Schumb, Peters and Milligan (24) realized that the increase in damage rate with temperature is most probably due to decrease in solubility of the gases. They also reasoned that at higher temperatures the vapor of the liquid itself would act as permanent gas, thereby cushioning out the bubble collapse energy. Recently, Bebchuk and Rozenberg (25) showed that the solubility of gases in the liquid is one of the most important parameters controlling damage. By increasing the solubility of gases in water equal to that found in ethyl alcohol, they obtained the same order of magnitude of damage in both liquids. Devine and Plesset (26) gave an empirical factor, D which behaves in the same manner as the damage observed in water at various temperatures.

$$D = \left[1 - \frac{p_v(T)}{p_v(100)}\right] \frac{C_s(0)}{C_s(T)} \qquad [11]$$

where

$p_v(T)$ - vapor pressure at any temperature T

$p_v(100)$ - vapor pressure at 100°C

$C_s(0)$ - concentration of dissolved air at 0°C

$C_s(T)$ - concentration at any temperature T.

More recently Leith (27) also devised an empirical formula for predicting damage in various liquids at various temperatures as follows.

$$\frac{W_\ell}{W_w} = 0.6 \frac{\rho_\ell \, V_w \, \sigma_\ell}{\rho_w \, V_\ell \, \sigma_w} \left[\frac{P_a - p_w}{P_a - p_\ell}\right]^{10} \qquad [12]$$

where

W - weight loss

ρ - density

V - viscosity

σ - surface tension

p - vapor pressure

P_a - atmospheric pressure

Subscripts w and ℓ stand for water and any alkali liquid metal respectively. Leith apparently arrived at this empirical relationship by fitting the data he obtained for water, sodium-potassium alloy and gasoline. The basic weakness with this approach is that it is not based on any physical meaning to the

function of each of the properties included in this formula. In our view, two important parameters controlling the dynamics of bubble collapse are omitted. They are

1. The velocity of sound in the liquid.
2. The solubility of gases in the liquid.

In the experiments with magnetostriction oscillators (from which Leith obtained the data), the pressure amplitude is of the order of $\rho_\ell C_\ell U_o$ (28) where ρ_ℓ is the density of the liquid, C_ℓ is the velocity sound in the liquid and U_o is the maximum velocity of the test specimen in the liquid. The bubble growth and collapse is caused by this pressure field which is proportional to the velocity of sound in the liquid. Similarly the solubility of gas in the liquid is very important since it controls the damping of bubble collapse intensity. The omission of these two parameters is a very serious drawback in understanding the effect of temperature on cavitation damage. Furthermore the changes in mechanical properties of the materials at various temperatures are very important in predicting weight loss which Leith ignores completely.

The above discussion points out that the present understanding of the role of various properties of the liquids at various temperatures is only qualitative. It is not presently possible to extrapolate the data in a quantitative manner. This development must await an understanding of the intensity of bubble collapse and how it varies with other parameters. However the present experiments have shown that the relative intensity

of damage in liquid sodium at 1500°F is of the order of 10^{-3} as compared to 1 at 400°F.

Effect of Oxide Content in Liquid Sodium on Cavitation Damage

In this program the effect of oxide content in the liquid sodium was investigated since it is known that the corrosion resistance of certain refractory alloys in liquid metals can be decreased markedly with increasing oxide contamination (Reference 24). By deliberately adding Na_2O_2 to the hot liquid sodium, the O_2 content was increased to 100 ppm as compared to the purity of ~30 ppm achievable in the test facility*. Cavitation damage tests on 316 stainless steel and on TZM were conducted at the 100 ppm O_2 level at 1000°F and at 1500°F. The results of these experiments (Figure 13) show that this level of oxide impurity does not have any noticeable effect on the cavitation damage resistance of these two metals at these two temperatures during the relatively short testing time. Further work is necessary to determine if higher levels of O_2 contamination or larger exposure times have a deleterious effect on the cavitation damage resistance of a given material.

* Originally, sufficient weight percent of oxide was added to increase oxide contamination to 200 ppm. However, it is believed that upon decomposition of the Na_2O_2 some oxide was trapped in the sodium vapor above the liquid level in the closed retort.

2. High Frequency Fatigue Tests

To understand the relationship between the cavitation damage resistance and the environmental fatigue behavior of metals, high frequency fatigue tests on 316 stainless steel and TZM were conducted in liquid sodium at two temperatures (1000°F and 1500°F). The technique employed for these tests has already been described in this report. The fatigue specimen was immersed in liquid sodium at the required temperature and vibrated at a selected stress level. The time for failure was noted. The frequency of vibration was recorded by a frequency counter while the stress level was monitored by means of a calibrated voice coil whose sinusoidal voltage was displayed on an oscilloscope.

Effect of Liquid Sodium Temperature on Fatigue

Figures 21 through 24 show the results of these fatigue tests at two temperatures. As expected, the fatigue strength for the two metals tested decreases very much with increasing temperature. While the results for 316 stainless steel are very good, a large scatter of the data for TZM is observed. This can possibly be accounted for by (a) the cold working properties, (b) the possibility of machining irregularities and (c) the relative inhomogeneity of the metal. The TZM specimens were prepared from 1/2 inch diameter rod stock which was initially stress relieved for 1/2 hour at 2250°F. However, no further heat treatment was applied after machining and polishing the fatigue specimens.

Effect of Frequency on Fatigue

The present fatigue tests were conducted at a frequency of 14 kcs (nearly) which is the same frequency utilized for cavitation damage tests in order to determine if strain rate effects are predominant under this type of dynamic loading. The results of these tests would be more useful if some comparison could be made with conventional fatigue tests. Danek and Achter (Reference 30) tested 316 stainless steel at 1500°F in 3×10^{-5} torr vacuum by means of a specially constructed fatigue machine. They used both mechanical drive (oscillating permanent magnets) and electromagnetic drive (alternate excitation). The frequency of their test was of the order of 4 to 5 cps as compared to the 14000 cps of the present experiments. Figure 22 shows the data of Danek and Achter as well as the present high frequency fatigue data in 1500°F sodium at 14000 cps. It seems that the strain rate effects at these temperatures are not significant.

Effect of Oxide Content in Liquid Sodium on Fatigue

Further fatigue experiments were conducted to evaluate the effect of oxide content in liquid sodium. All the results discussed earlier were obtained in sodium with ~30 ppm O_2 level while some of the results shown in Figures 21 through 24 were obtained in liquid sodium with ~100 ppm O_2 level at two temperatures. As is evident from these results, no perceptible effect was noticed at this oxide level for the short test duration employed.

3. Stress Corrosion Tests

Effect of Temperature of Liquid Sodium on Stress Corrosion

The stress corrosion specimens described previously were tested at approximately 50, 75 and up to near 100 percent yield for 316 stainless steel and TZM and were immersed in liquid sodium (with oxide levels of ~30 ppm) at two temperatures (1000°F and 1500°F) up to 60 hours. The arrangement for these tests is shown in Figure 25. No stress corrosion cracks were observed even with a 20 power microscope for all cases. Observations were made at the axis of maximum fiber stress with the specimens restressed to near 100 percent yield.

Effect of Oxide Content in Liquid Sodium on Stress Corrosion

The same experiments were repeated in liquid sodium with an oxide content of ~100 ppm. Even in this case no stress corrosion cracking was observed up to 60 hours. Figures 26 and 27 are photographs of 316 stainless steel and TZM specimens exposed at 1500°F at near 100 percent yield stress.

The results of the high frequency fatigue tests and the stress corrosion tests failed to show anomalous behavior of 316 stainless steel despite the high rates of strain, high static stresses or high oxide contamination. These preliminary results indicate that the strain energy correlating parameter suggested need not be modified for 316 stainless steel. In the case of TZM alloy, no conclusions could be drawn for the fatigue tests

since no comparative data were available at low frequency. However, oxide contamination in both fatigue and stress corrosion tests did not alter its behavior.

VI. CONCLUSIONS

The following conclusions may be drawn from the results of these investigations:

1. Relative cavitation damage resistance exhibited by the five high temperature alloys tested in this program depends upon the zone of damage in which the comparison is made.

2. Among the metals tested, Stellite 6B seems to possess the best cavitation damage resistance although the rate of damage in the steady zone was not determined.

3. The rate of damage for 316 stainless steel decreases with increasing temperature up to 1500°F.

4. A comparison between the fatigue data at 4-5 cps using 316 stainless steel in 3×10^{-5} torr vacuum at 1500°F and the fatigue data at 14000 cps for the same metal in 1500°F liquid sodium shows little deviation between the two results. This result seems to indicate the absence of strain rate effects and corrosion fatigue effects in the present fatigue tests for 316 stainless steel in liquid sodium.

5. The stress corrosion tests (constant strain) on 316 stainless steel and on TZM at 1000°F and 1500°F in liquid sodium up to a stress of 100 percent yield did not show any cracking over a test period of 60 hours.

6. Over the short test period used, an increase in oxide content in liquid sodium from ~35 ppm to ~100 ppm does not essentially change the high frequency fatigue or stress corrosion properties of 316 stainless steel or of TZM at 1000°F and at 1500°F.

REFERENCES

1. P. G. Smith, J. H. De Van, and A. G. Grindell, "Cavitation Damage to Centrifugal Pump Impellers During Operation with Liquid Metals and Molten Salt at 1050-1400°F," Am. Soc. Mech. Engrs., Paper No. 62-Hyd-2, Jour. Basic Engr., September 1963.

2. R. S. Kulp, and M. V. Altieri, "Cavitation Damage of Mechanical Pump Impellers Operating in Liquid Metal Space Power Loops," NASA CR-165, NASA, Washington, D. C., July 1965.

3. H. S. Preiser, A. Thiruvengadam and C. Couchman, III, "Cavitation Damage in Liquid Sodium," HYDRONAUTICS, Incorporated, NASA CR-54072, April 1964.

4. H. S. Preiser, A. Thiruvengadam, and C. Couchman, III, "Cavitation Damage Research Facilities for High Temperature Liquid Alkali Metal Studies," ASME Symposium on Cavitation Research Facilities and Techniques, Philadelphia, Pa., May 1964.

5. C. Couchman, III, H. S. Preiser and A. Thiruvengadam, "Cavitation Damage in Liquid Metals," HYDRONAUTICS, Incorporated Technical Progress Report 467-1, NASA CR-54332, March 1965.

6. A. Thiruvengadam, H. S. Preiser and S. L. Rudy, "Cavitation Damage in Liquid Metals," HYDRONAUTICS, Incorporated Technical Progress Report 467-2, NASA CR-54391, April 1965.

7. A. Thiruvengadam, H. S. Preiser and S. L. Rudy, "Cavitation Damage in Liquid Metals," HYDRONAUTICS, Incorporated Technical Progress Report 467-3, NASA CR-54459, June 1965.

8. H. S. Preiser and A. Thiruvengadam, "Instrumentation for Evaluating Cavitation Damage Resistance and High Frequency Fatigue of Refractory Alloys in High Temperature Liquid Alkali Metals," Paper presented at the Liquid Metal Technology Conference, Argonne National Laboratory, Argonne, Illinois, September 1965.

9. A. Thiruvengadam, and H. S. Preiser, "On Testing Materials for Cavitation Damage Resistance," HYDRONAUTICS, Incorporated Technical Report 233-3, December 1963. (See also Jour. Ship Research, Vol. 8, No. 3, December 1964).

10. W. P. Mason, "Internal Friction and Fatigue in Metals at Large Amplitudes," Jour. Acoust. Soc. of America., Vol. 28, No. 6, pp. 1207-1218, 1956.

11. E. A. Neppiras, "Techniques and Equipment for Fatigue Testing at Very High Frequencies," Proc. ASTM, Vol. 59, pp. 691-709, 1959.

12. A. Fox, "A Comparison of Ultrasonic and Conventional Axial Fatigue Tests on Aluminum Alloy Rod," Materials Research and Standards, pp. 60-63, February 1965.

13. A. Thiruvengadam, "High Frequency Fatigue of Metals and Their Cavitation Damage Resistance," HYDRONAUTICS, Incorporated Technical Report 233-6, December 1964.

14. T. Lyman, Ed., C. H. Gerlach, Assoc. Ed. Metals Handbook, 1956 Supplement. The Am. Soc. for Metals, P. 98, 1954.

15. S. Timoshenko, "Strength of Materials," Part I, D. Van Nostrand Company, Inc., Third Edition, p. 378, 1955.

16. A. Thiruvengadam, "A Comparative Evaluation of Cavitation Damage Test Devices," HYDRONAUTICS, Incorporated Technical Report 233-2, November 1963. (See also Symp. Cavitation Research Facilities and Techniques, ASME, New York, May 1964).

17. P. Eisenberg, H. S. Preiser and A. Thiruvengadam, "On the Mechanisms of Cavitation Damage and Methods of Protection," Society of Naval Arch. and Marine Engrs., Winter Annual Meeting, New York, November 1965.

18. P. Eisenberg, "Cavitation Damage," HYDRONAUTICS, Incorporated Technical Report 233-1, December 1963.

19. A. Thiruvengadam, "A Unified Theory of Cavitation Damage," Trans. ASME., Vol. 85, Series D, No. 3, Jour. Basic Engr., pp. 365-376, September 1963.

20. A. Thiruvengadam, and S. Waring, "Mechanical Properties of Metals and Their Cavitation Damage Resistance," HYDRONAUTICS, Incorporated Technical Report 233-5, June 1964.

21. A. Thiruvengadam, C. Couchman, III and H. S. Preiser, "Cavitation Damage Resistance of Materials in Liquid Sodium," AIAA First Annual Meeting and Display 1964, Washington, D.C., (See also Jour. Spacecraft and Rockets, AIAA, Vol. 2,No. 2, 1965, 267-269).

22. S. G. Young and J. R. Johnston, "Accelerated Cavitation Damage of Steels and Super Alloys in Liquid Metals," NASA Technical Note NASA TN D-3426, National Aeronautics and Space Administration, Washington, D. C., May 1966.

23. A. Thiruvengadam, "Intensity of Cavitation Damage Encountered in Field Installations," HYDRONAUTICS, Incorporated Technical Report 233-7, February 1965. (See also Proc. Symp. on Cavitation Problems in Fluid Machinery, ASME Winter Annual Meeting, Chicago, Ill., November 1965).

24. W. C. Schumb, H. Peters and L. H. Milligan, "A New Method for Studying Cavitation Erosion of Metals," Metals and Alloys, pp. 126-131, May 1937.

25. A. S. Bebchuk and L. D. Rozenberg, "Dependence of Cavitation Erosion on the Solubility of a Gas under a Liquid," Soviet Physics Acoustics, pp. 496-498, October - December 1960.

26. R. E. Devine and M. S. Plesset, "Temperature Effects in Cavitation Damage," Dept. of Engr. and App. Sc., California Inst. Tech., Pasedena, California. Report No. 85-27, April 1964.

27. W. C. Leith, "Prediction of Cavitation Damage in the Alkali Liquid Metals," American Society for Testing Materials, Proc. 65, 789-800 (1965).

28. P. M. Morse, "Vibration and Sound," McGraw-Hill Book Company, Inc., New York, 1948 (sec. ed.) p. 534.

29. J. R. De Stefano and A. P. Litman, "Effects of Impurities in Some Refractory Metal-Alkali Metal Systems," Corrosion, Vol. 20, No. 12, pp. 392-399, 1964 (December).

30. G. J. Danek, Jr., and M. R. Achter, "A High Temperature Vacuum and Controlled Environment Fatigue Tester," ASTM Bulletin No. 234, pp. 48-52, December 1958.

TABLE 1

Test Parameters of High Frequency Fatigue Specimens

Metal	Temp. (^{o}F)	Wave Length (Inches)	Modulus of Elasticity (psi x 10^{-6})	Specimen Length (Inches)	Resonant Frequency (cps)
316 stainless steel	1000	12.2	21.8	5.500	14140
	1500	11.3	18.5	5.125	14080
TZM	1000	15.0	42.0	7.000	13990
	1500	14.5	39.0	6.750	14080

TABLE 2

Intensity of Cavitation Damage as a Function of Temperature in Liquid Sodium and 316 Stainless Steel

$I = W \cdot S_e \times 2.9 \times 10^{-6} \frac{\text{Watts}}{\text{Meter}^2}$; W - mgs/hours; S_e-psi

Temp.	Weight Loss* mg/hour	Strain Energy psi x 10^{-3}	Intensity watts/meter^2	$\frac{I_T}{I_{400}}$
300	13	29.0	1.10	0.88
400	16	27.0	1.25	1.0
500	6	25.0	0.44	.35
600	3	23.5	0.20	.16
700	6	23.0	0.40	.32
800	6	22.0	0.38	.30
900	-	21.0	0.24	.19
1000	2	20.0	0.12	196×10^{-1}
1100	0.70	19.0	0.04	$.32 \times 10^{-1}$
1200	0.25	16.5	0.012	$.96 \times 10^{-2}$
1300	0.70	13.5	0.027	$.22 \times 10^{-1}$
1400	0.50	11.5	0.017	$.14 \times 10^{-1}$
1500	0.01	10.0	0.003	$.24 \times 10^{-2}$

* Average of three readings

TABLE 3

Nominal Chemical Compositions of Test Metals
Weight Percent

Material	Cr	Ni	Mo	C	Mn	P	S	Si	Fe
316 S.S.	16-18	11-14	2-3	.08	2.0	.03	.03	175	Bal.
	Ta	W	Mo	Zr	C	Cb			
Cb-132M	20	15	5	1	.1	Bal.			
	C	Ti	Zr	Ni	Fe	O_2	H_2	N_2	Mo
TZM	.016	.48	.08	<.001	<.001	<.002	<.0001	.0003	Bal.
	W	Hf	C	O_2	N_2	H_2	Ta		
T-222	9.02	2.72	.007	.0019	.0037	.00012	Bal.		
	Ni	Si	Fe	Mn	Cr	Mo	W	C	Co
Stellite 6B	3	2	3	2	30	1.5	4.5	1.1	Bal.

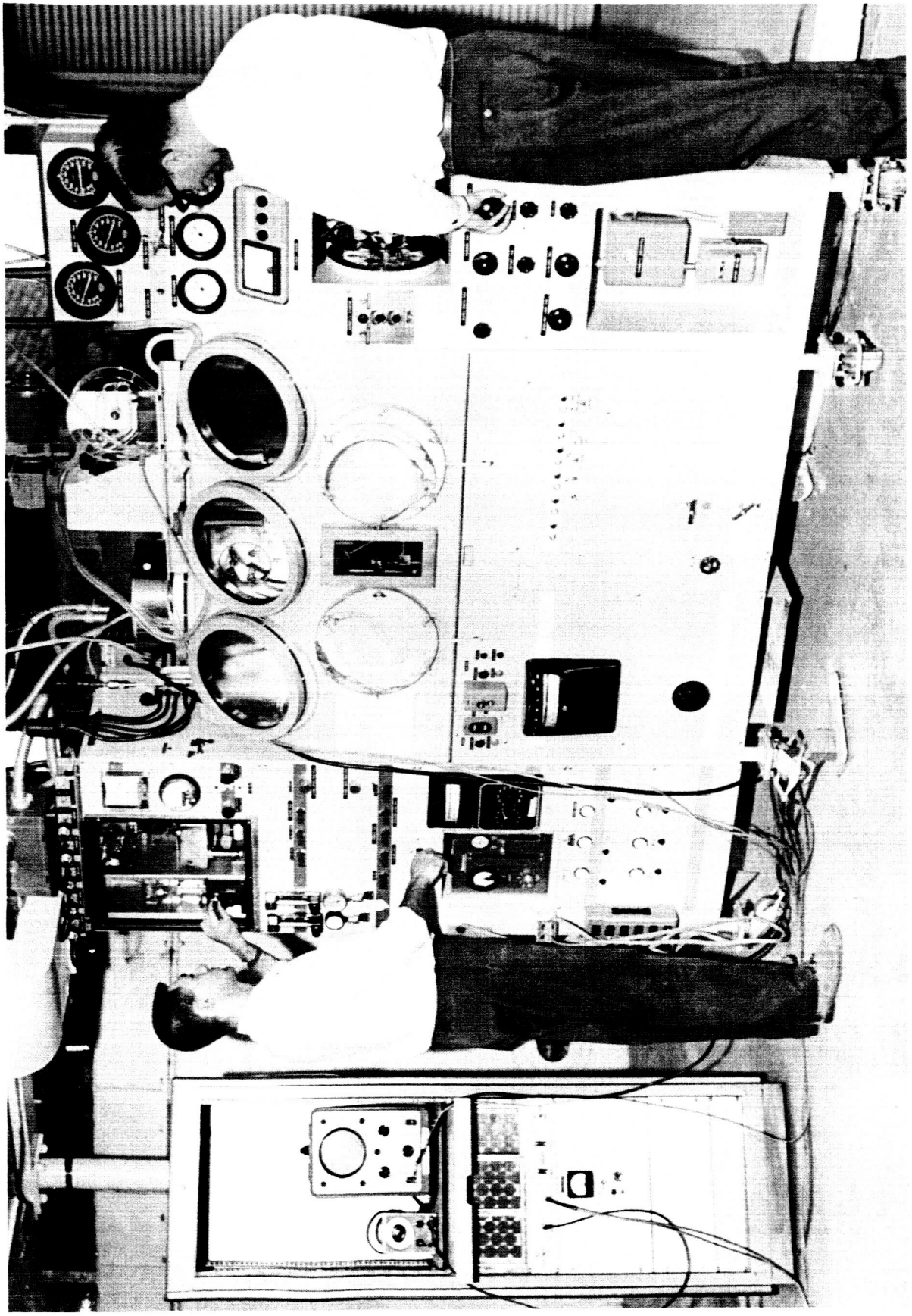

FIGURE 1 - HIGH TEMPERATURE ALKALI METAL TEST FACILITY

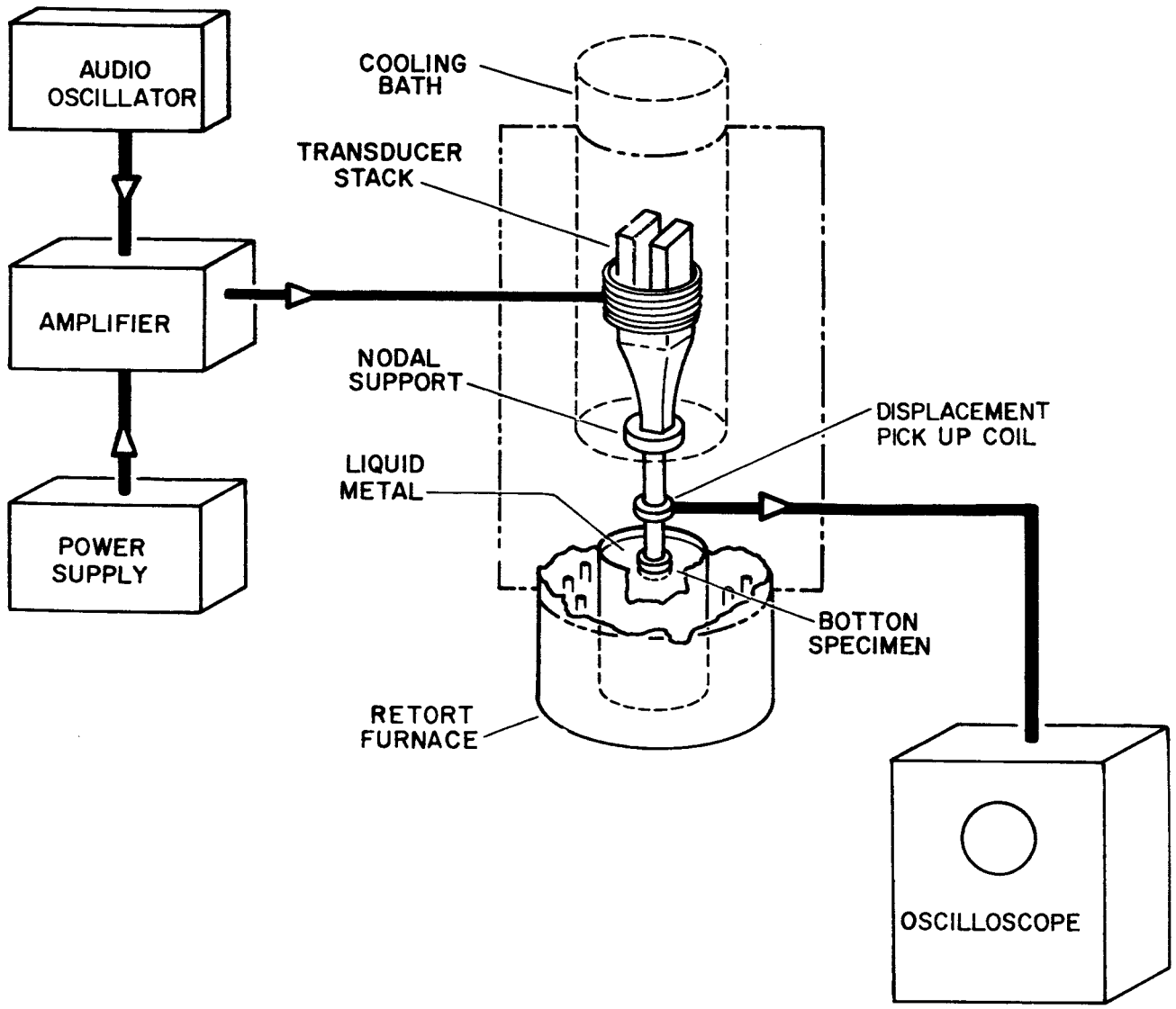

FIGURE 2 - BLOCK DIAGRAM OF THE MAGNETOSTRICTION APPARATUS USED FOR CAVITATION DAMAGE TESTS AND FOR HIGH FREQUENCY FATIGUE TESTS

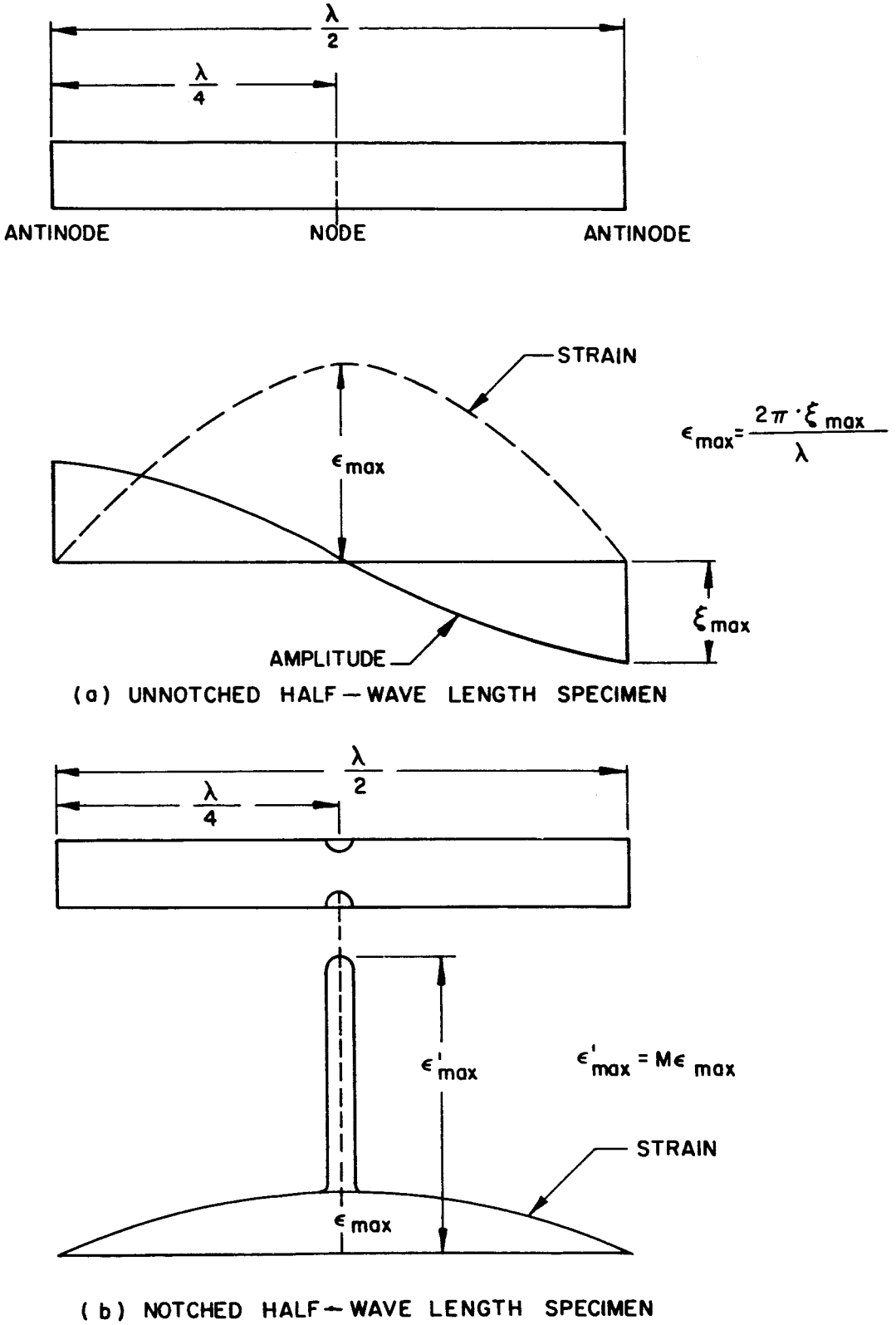

FIGURE 3 - BASIC PRINCIPLE OF HIGH FREQUENCY FATIGUE SPECIMEN DESIGN

NOTE:

1. GROOVE (DETAIL "A") IS TO BE SMOOTH, FREE FROM CHATTER TOOL MARKS, GROOVES OR OTHER DISCONTINUITIES. THE DIMENSIONS OF THE GROOVE MUST BE IDENTICAL FOR ALL SPECIMENS IN A LOT ±.001 AS MEASURED WITH AN OPTICAL COMPARATOR.
2. FINISH IN GROOVE 63 OR BETTER.
3. DIMENSION "A"=HALF WAVE LENGTH OF SOUND.

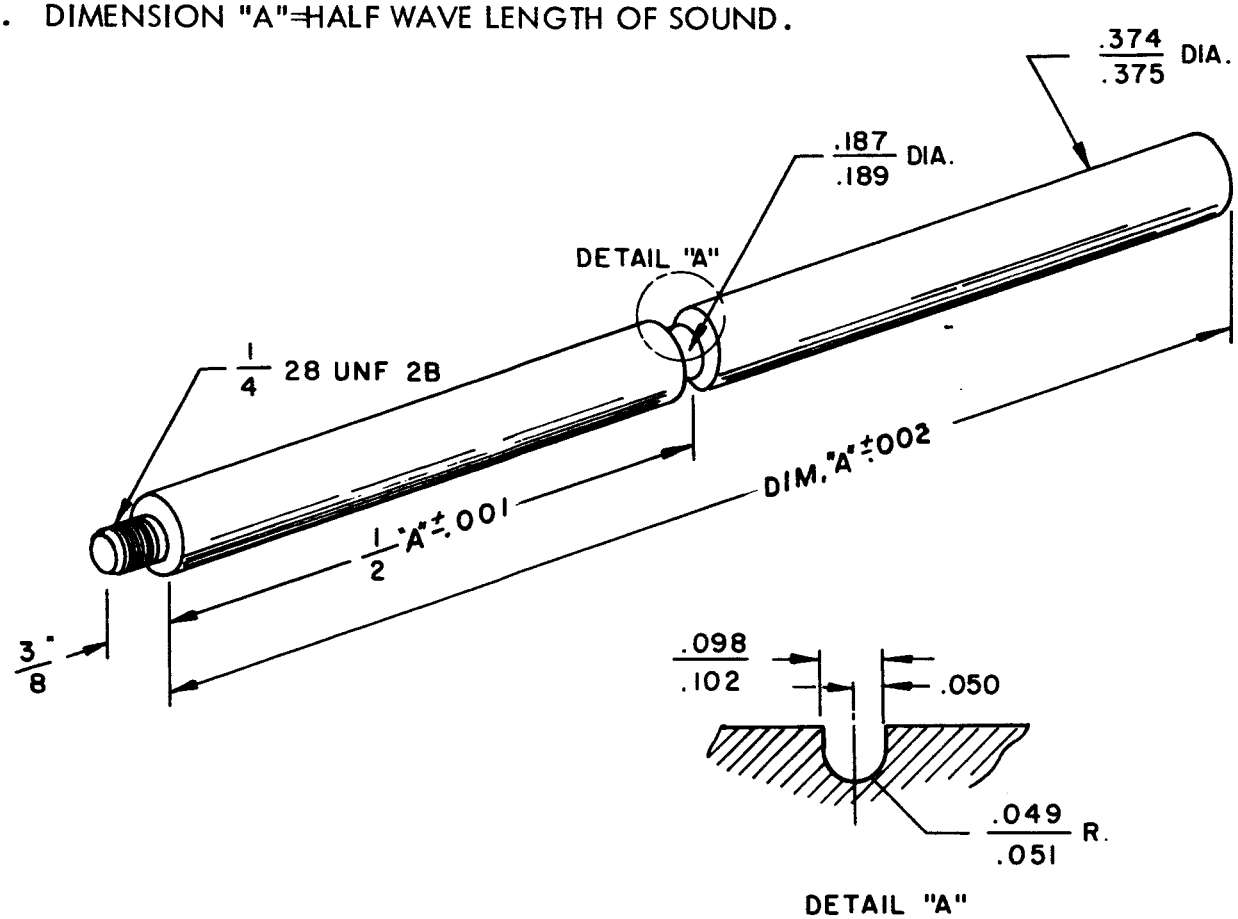

FIGURE 4 - HIGH FREQUENCY FATIGUE SPECIMEN

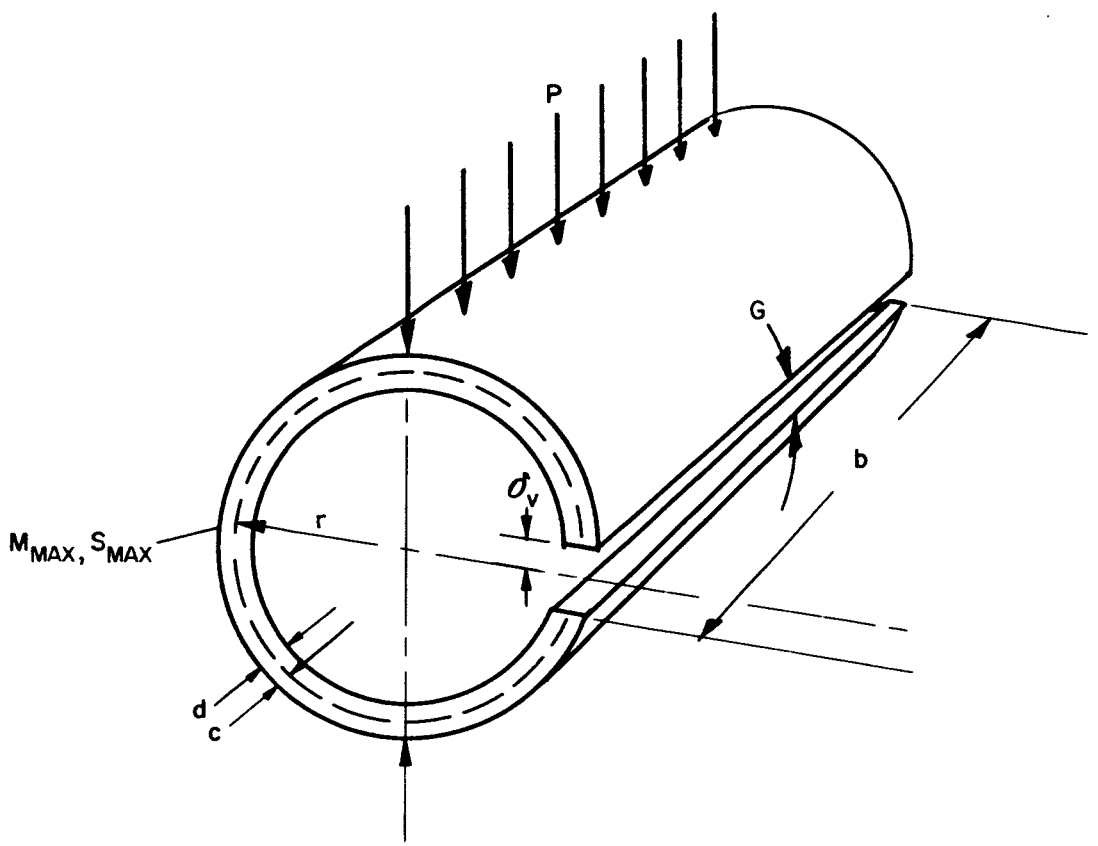

FIGURE 5 - SPLIT RING STRESS CORROSION SPECIMEN

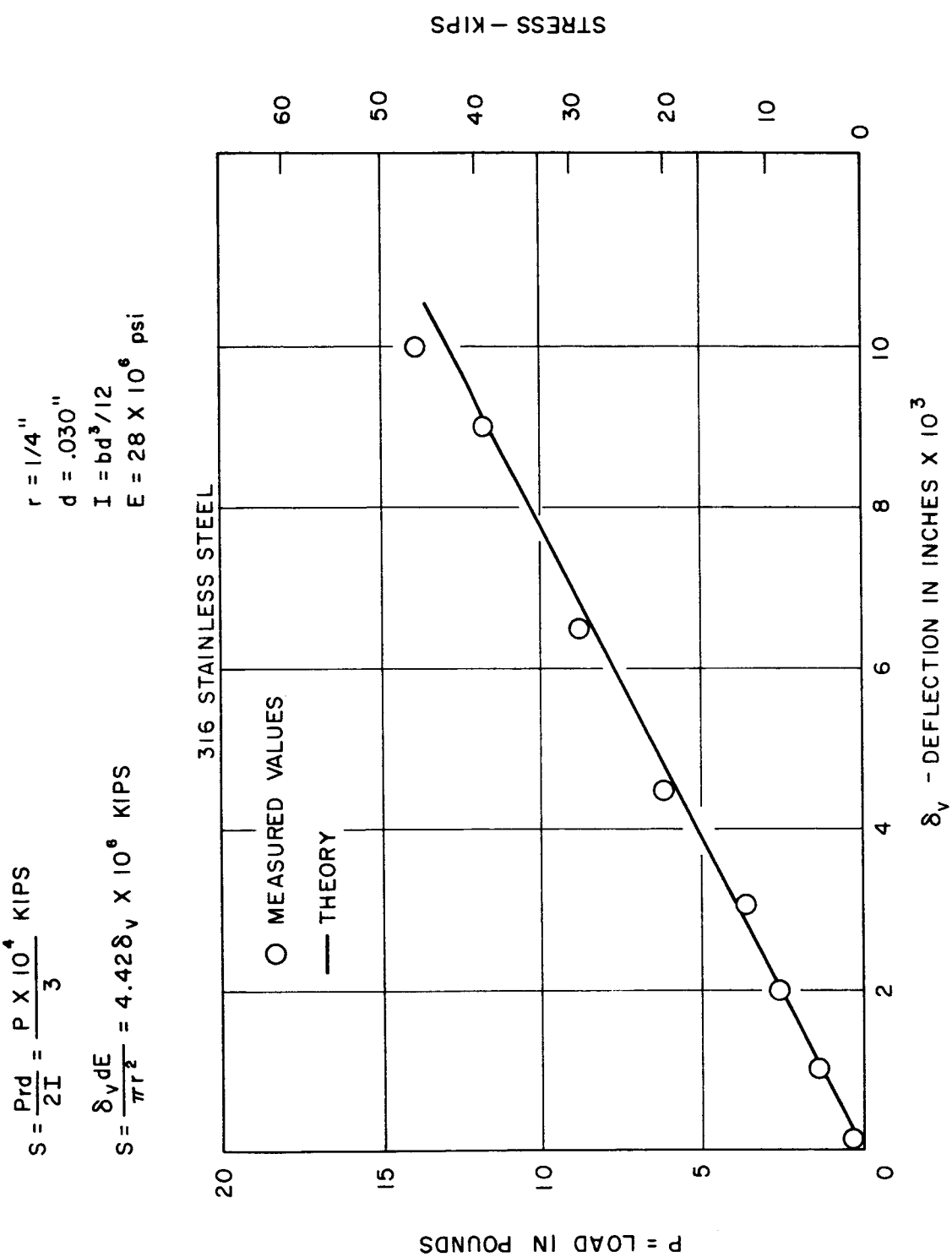

FIGURE 6 - CALIBRATION OF STRESS CORROSION SPECIMEN

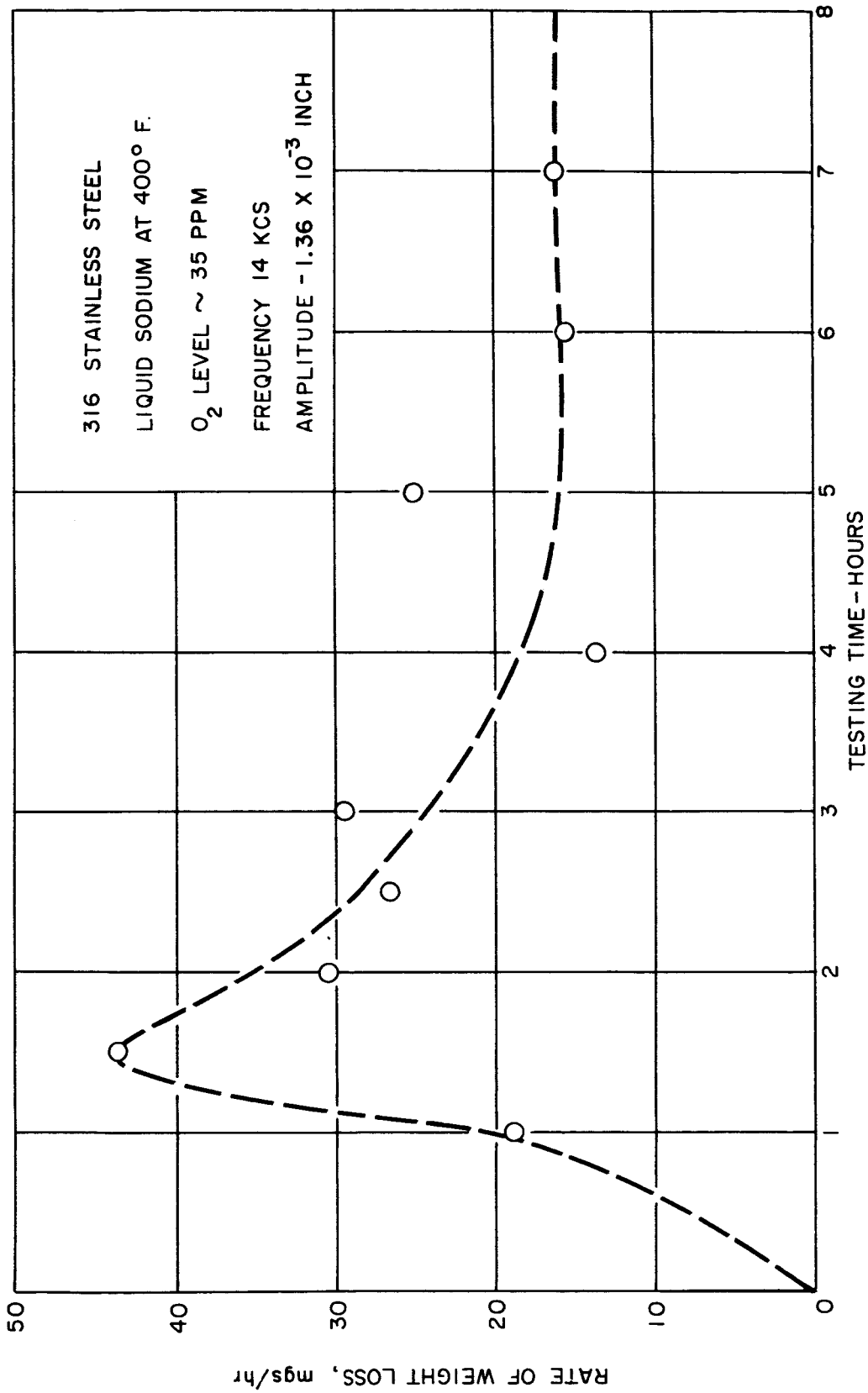

FIGURE 7 - EFFECT OF TESTING TIME ON CAVITATION DAMAGE RATE OF 316 STAINLESS STEEL

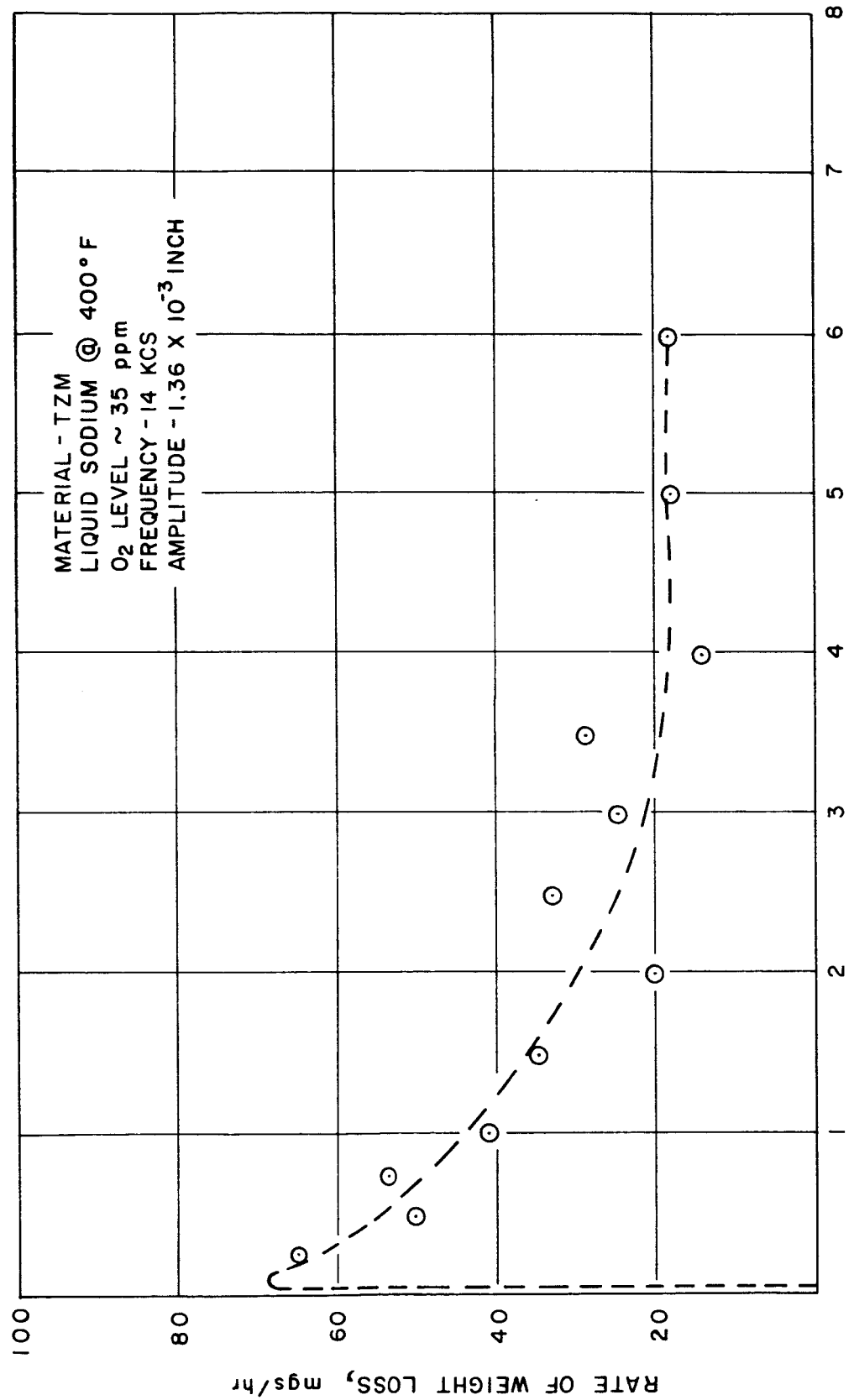

FIGURE 8 - EFFECT OF TESTING TIME ON THE RATE OF CAVITATION DAMAGE OF TZM

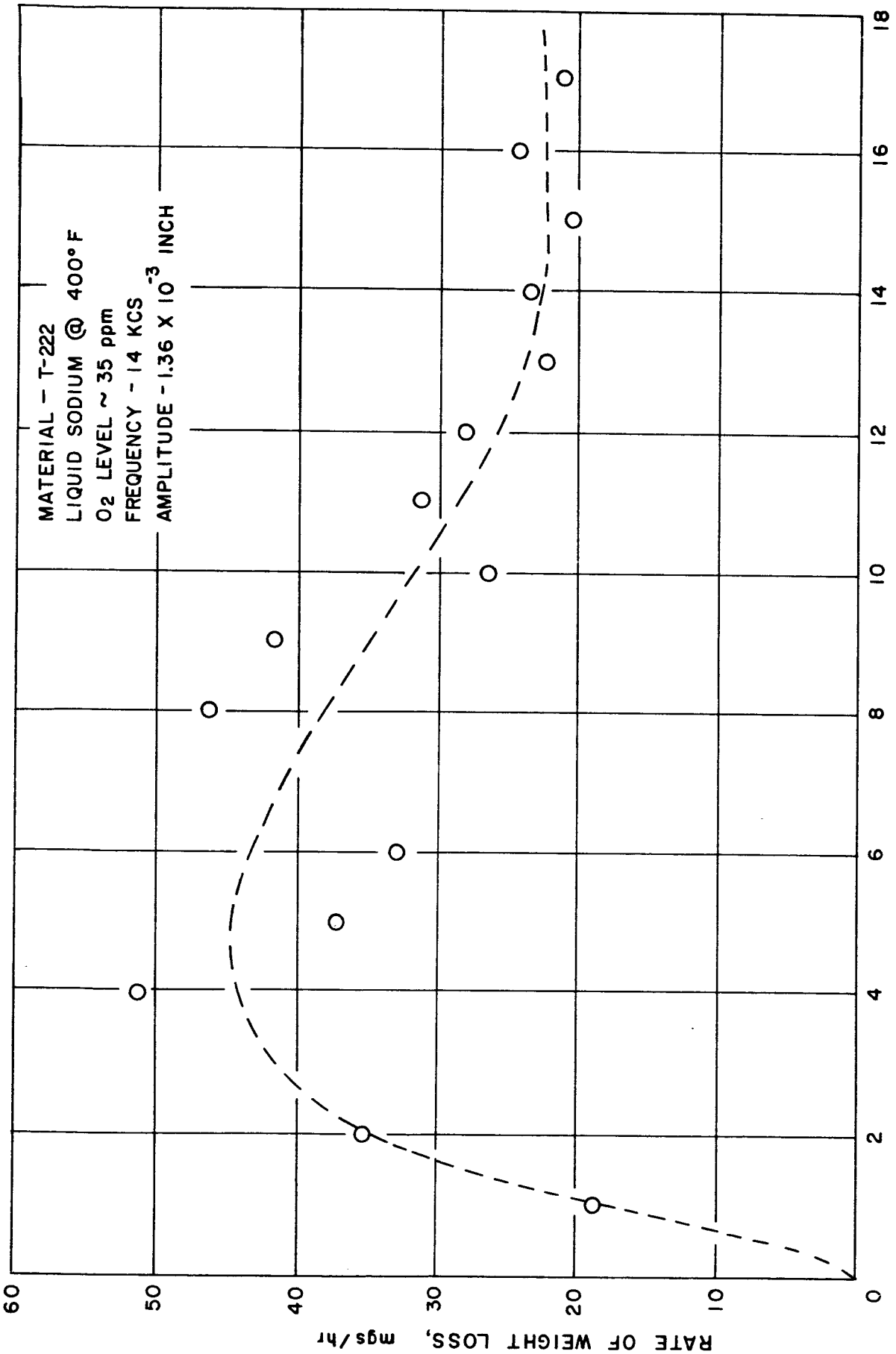

FIGURE 9 - EFFECT OF TESTING TIME ON THE RATE OF CAVITATION DAMAGE OF T-222

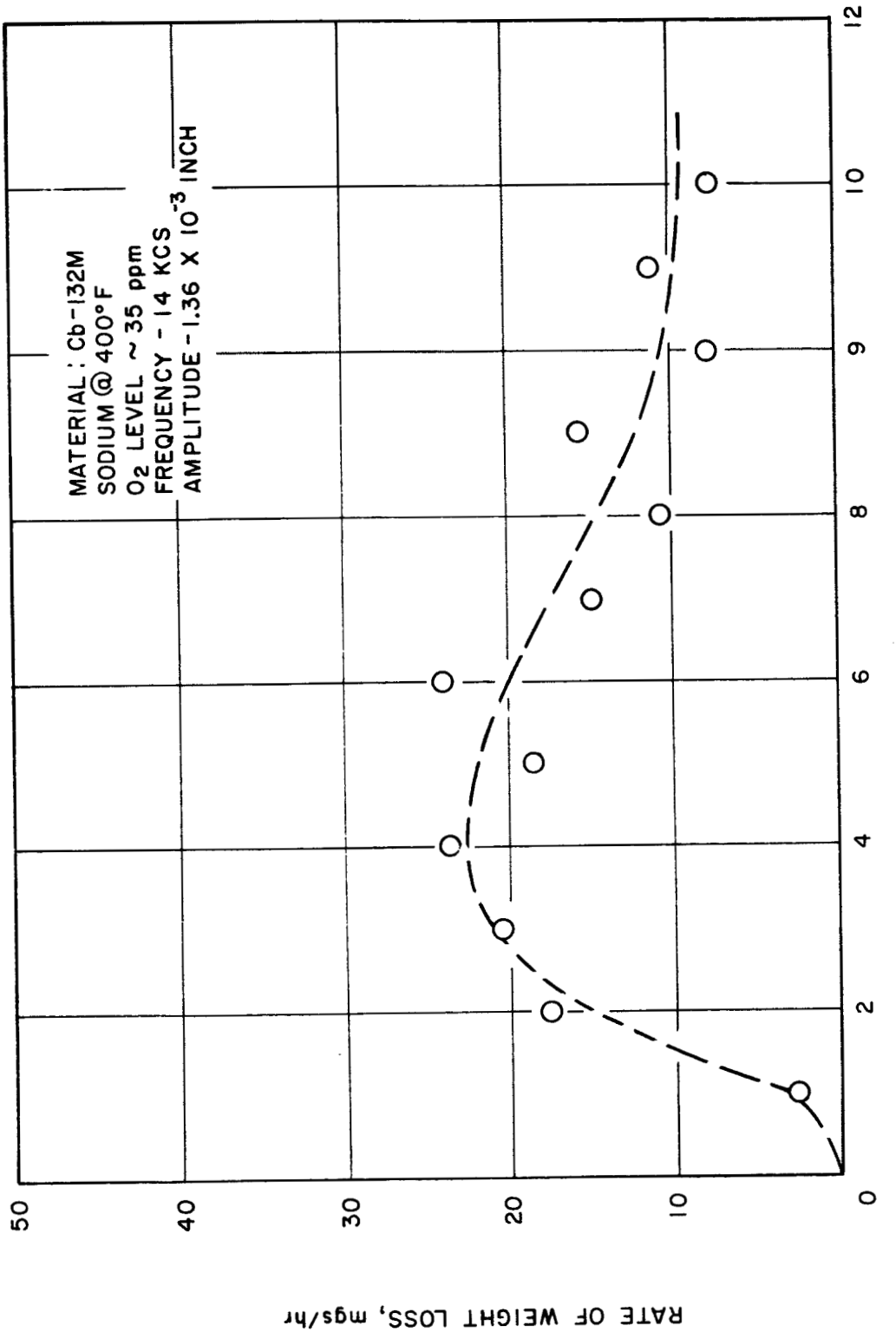

FIGURE 10 - EFFECT OF TESTING TIME ON THE RATE OF CAVITATION DAMAGE OF Cb-132M

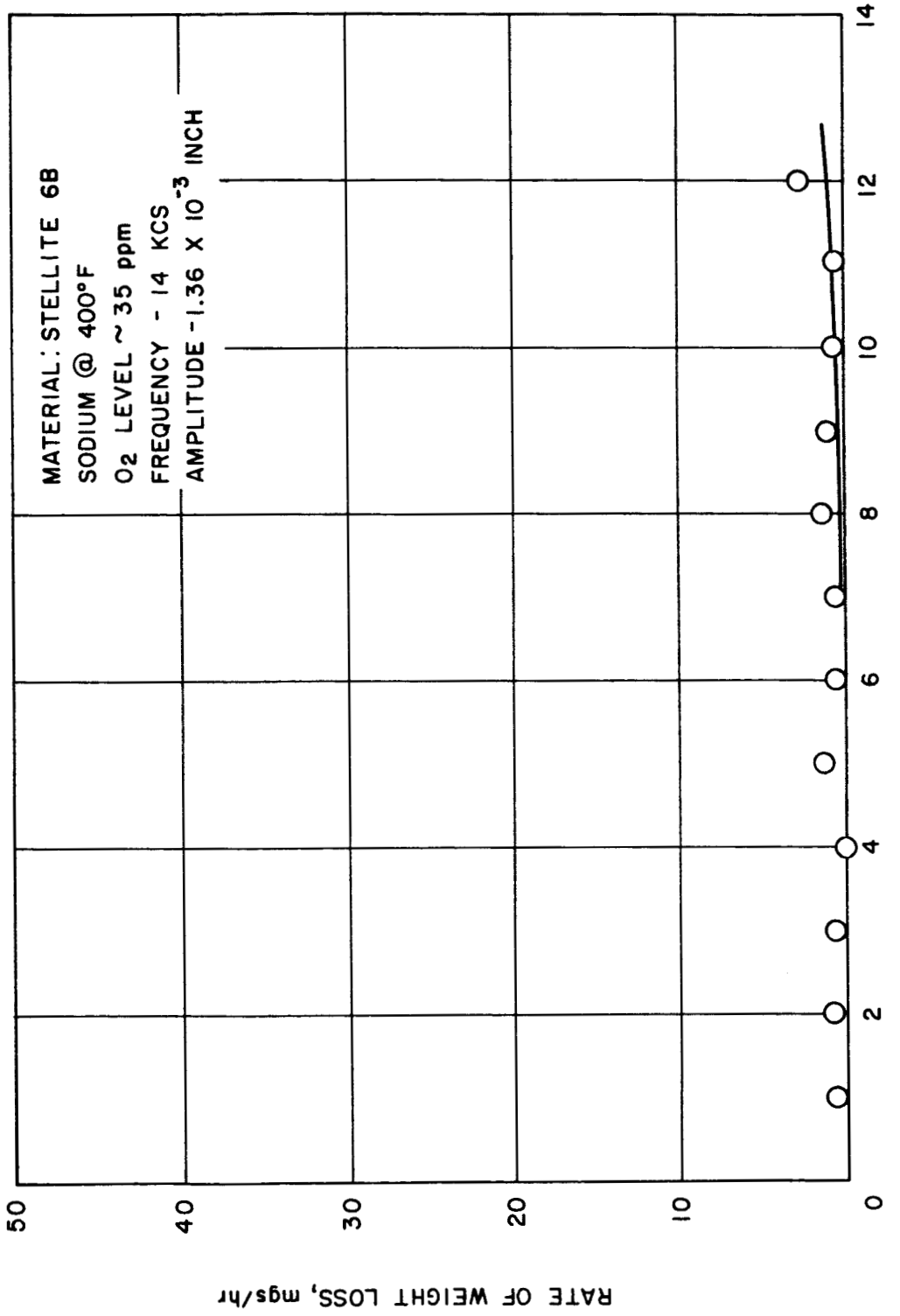

FIGURE 11 - EFFECT OF TESTING TIME ON THE RATE OF CAVITATION DAMAGE OF STELLITE 6B

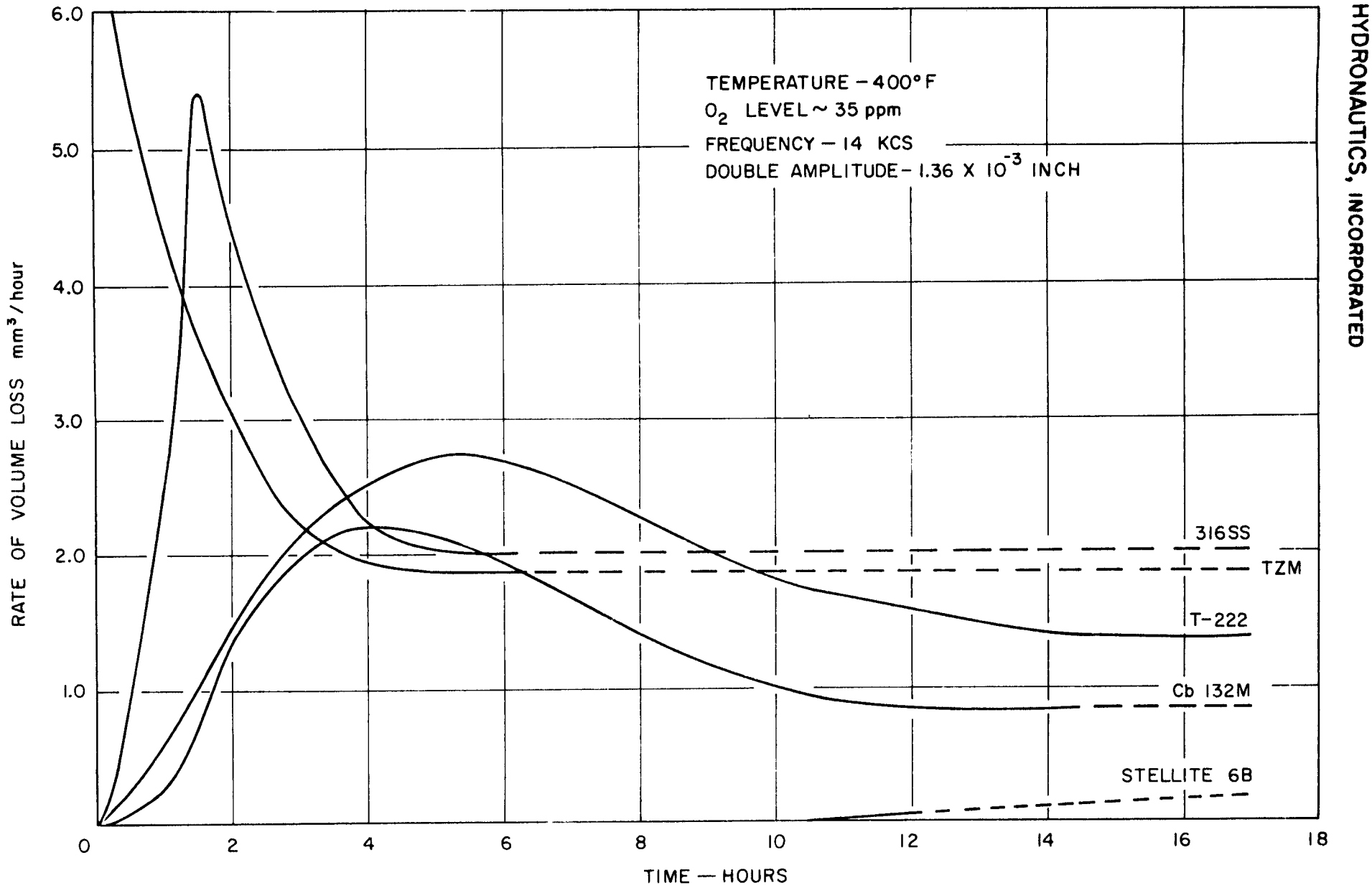

FIGURE 12 - RELATIVE CAVITATION DAMAGE RESISTANCE OF FIVE METALS TESTED IN 400°F SODIUM

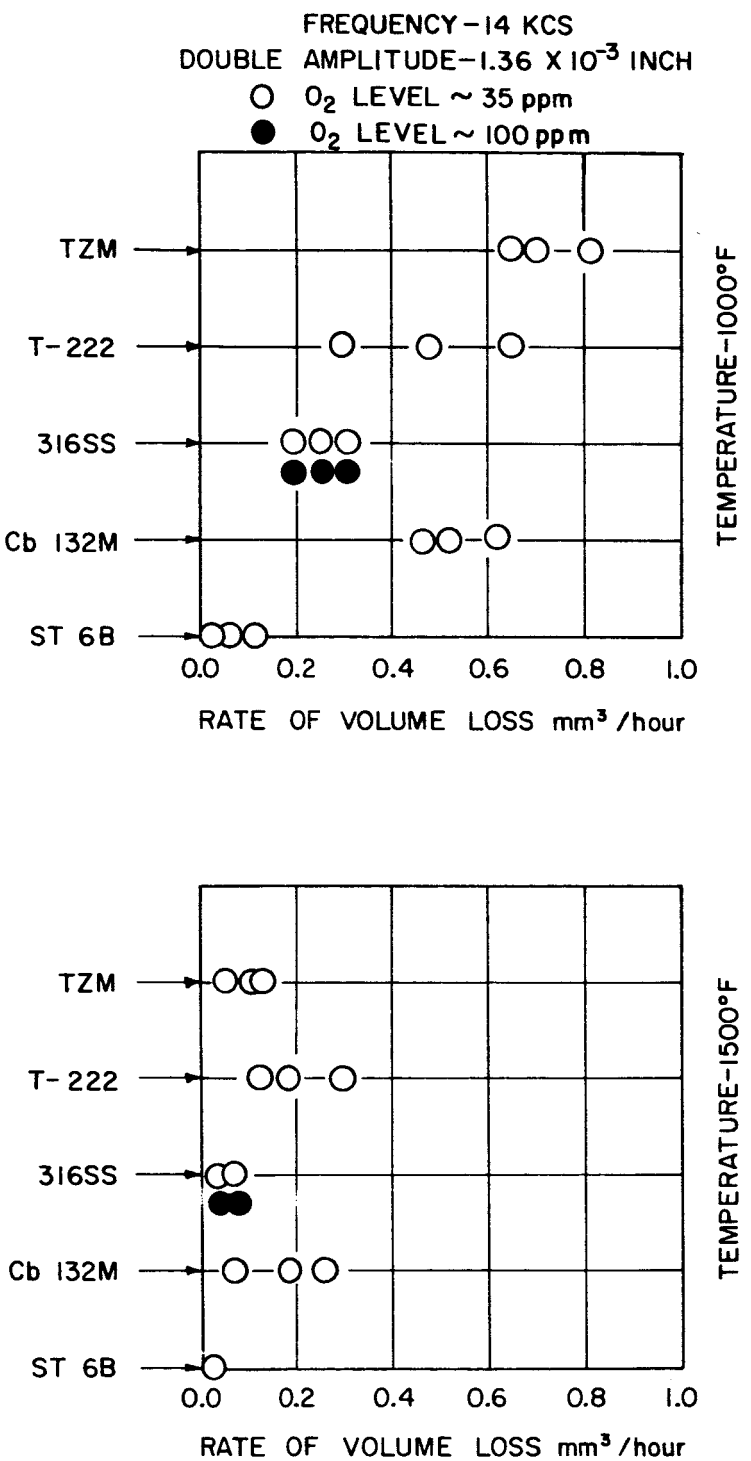

FIGURE 13 - CAVITATION DAMAGE RESISTANCE OF REFRACTORY ALLOYS IN HIGH TEMPERATURE LIQUID SODIUM (1000° AND 1500°F)

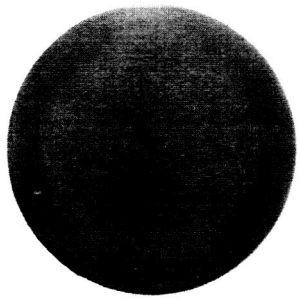

STELLITE 6B

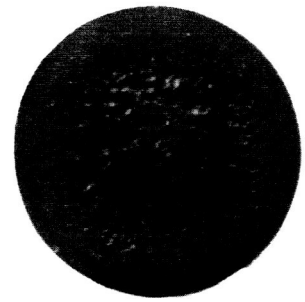

CB132

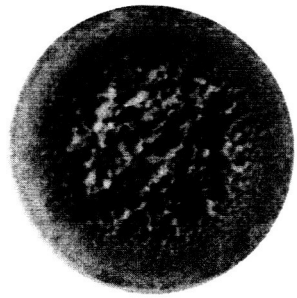

316 SS

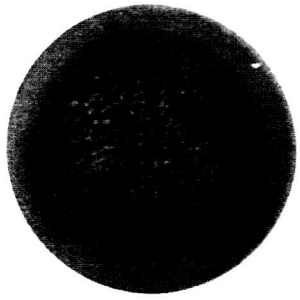

TZM

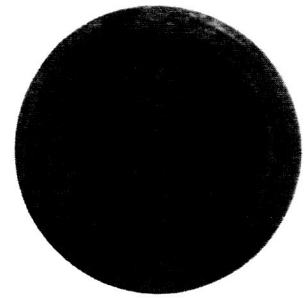

T-222

FIGURE 14 - PHOTOGRAPHS OF CAVITATION DAMAGE ON REFRACTORY METALS IN PURE LIQUID SODIUM ($0_2 \sim$ 35 ppm) UP TO 1500°F

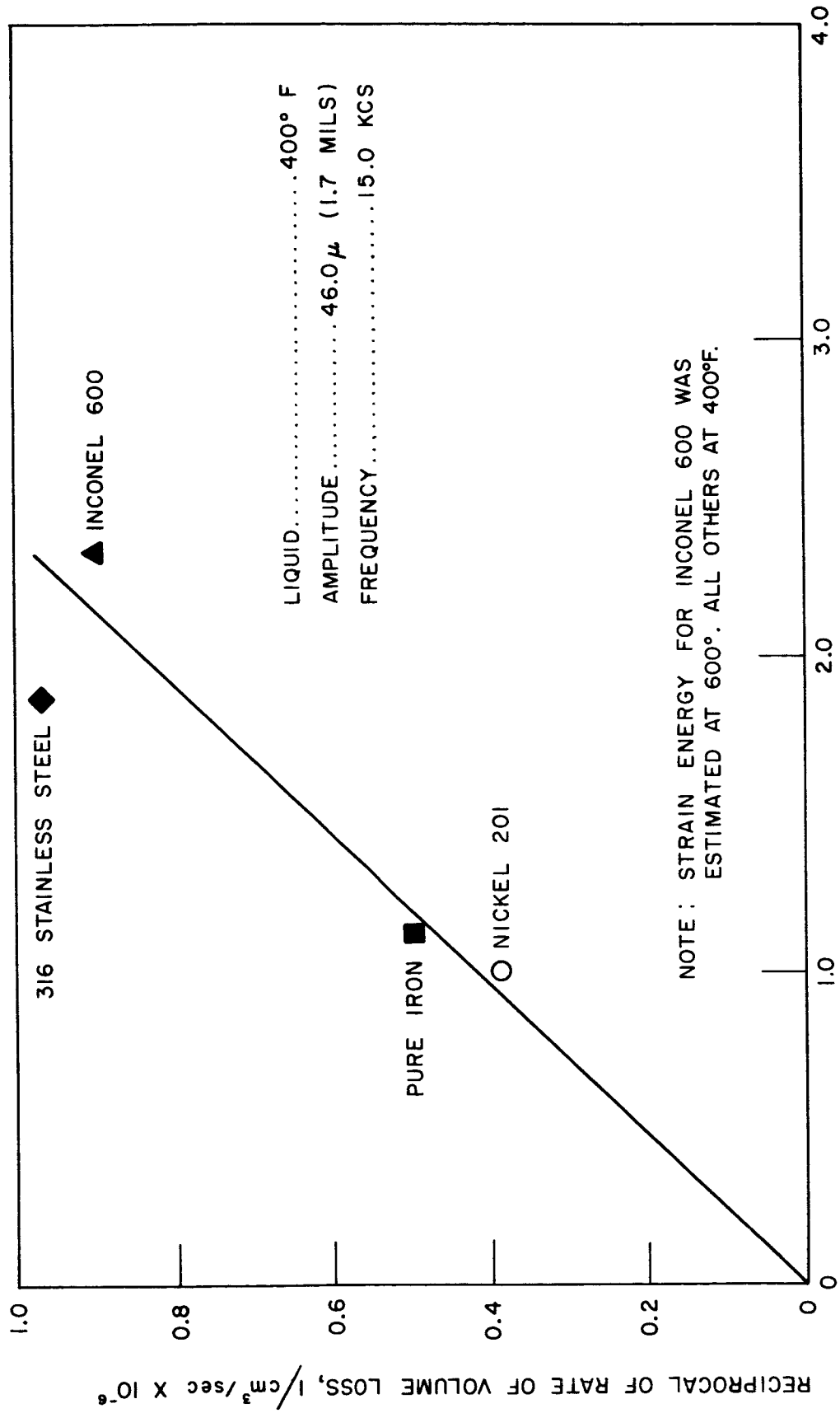

FIGURE 15 - RELATIONSHIP BETWEEN THE ESTIMATED STRAIN ENERGY AND THE RECIPROCAL OF THE RATE OF VOLUME LOSS IN 400°F IMPURE SODIUM (REF. 21)

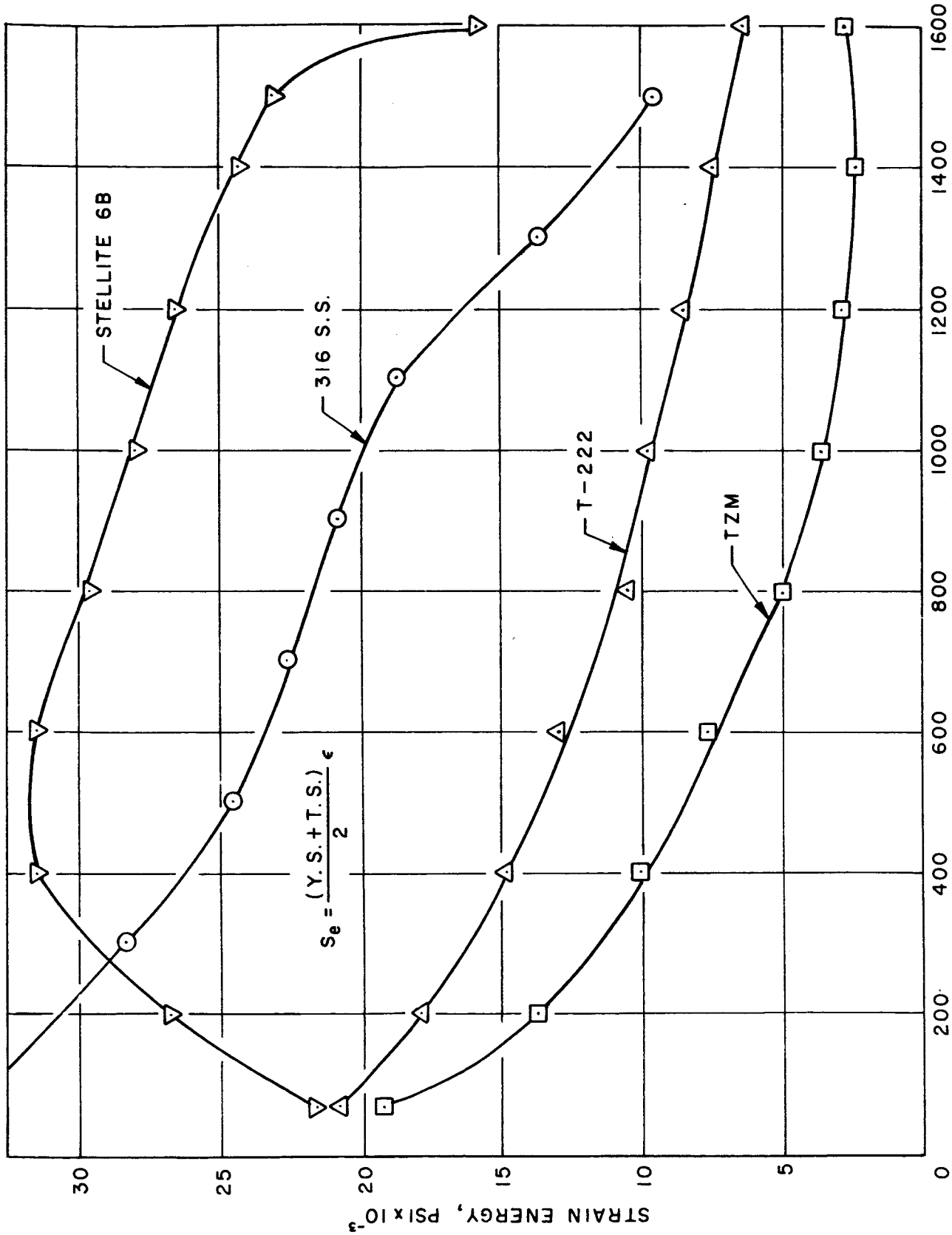

FIGURE 16 - EFFECT OF TEMPERATURE ON ESTIMATED STRAIN ENERGY

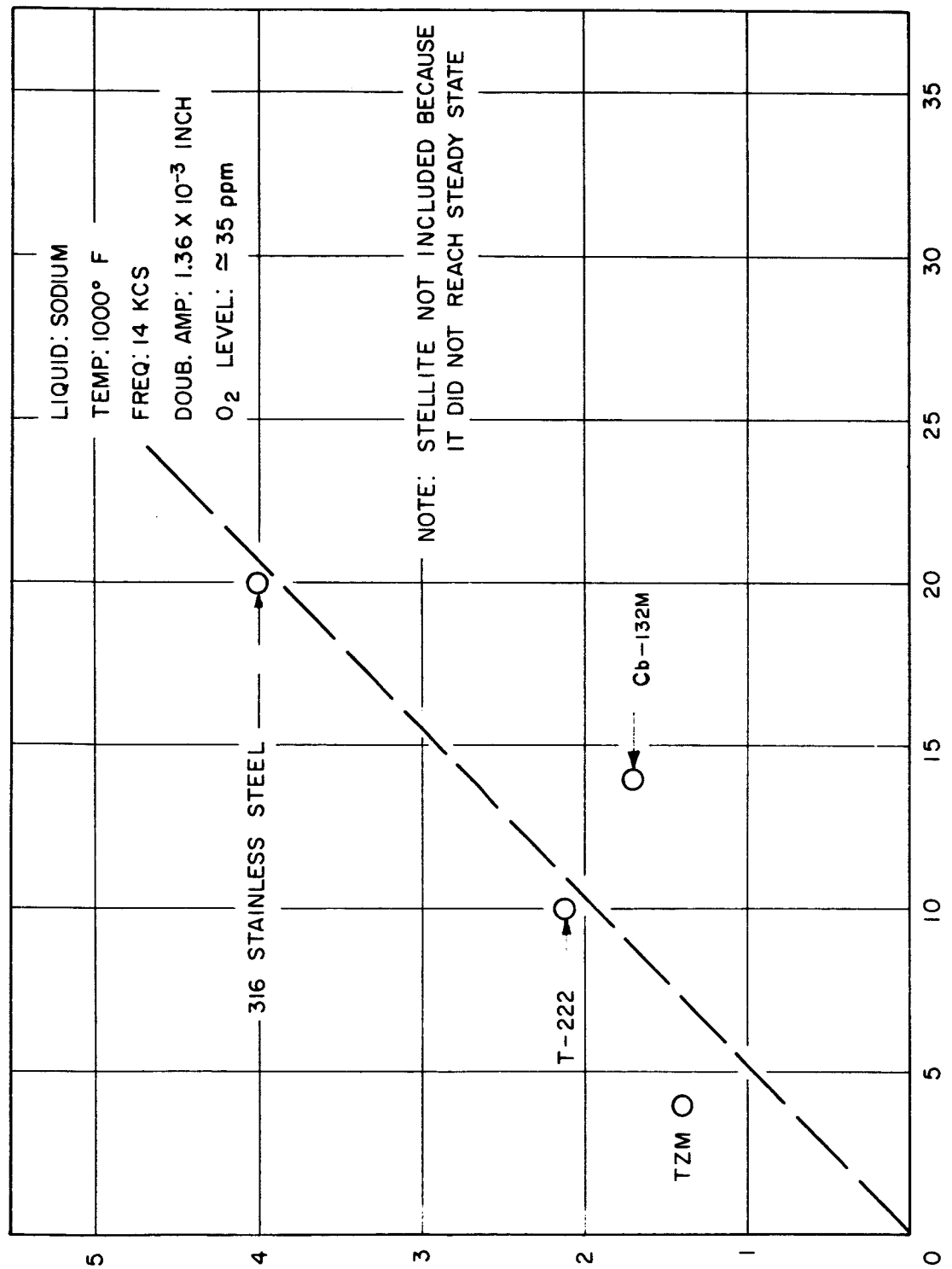

FIGURE 17 - RELATIONSHIP BETWEEN CAVITATION DAMAGE RESISTANCE AND ESTIMATED STRAIN ENERGY IN 1000°F LIQUID SODIUM

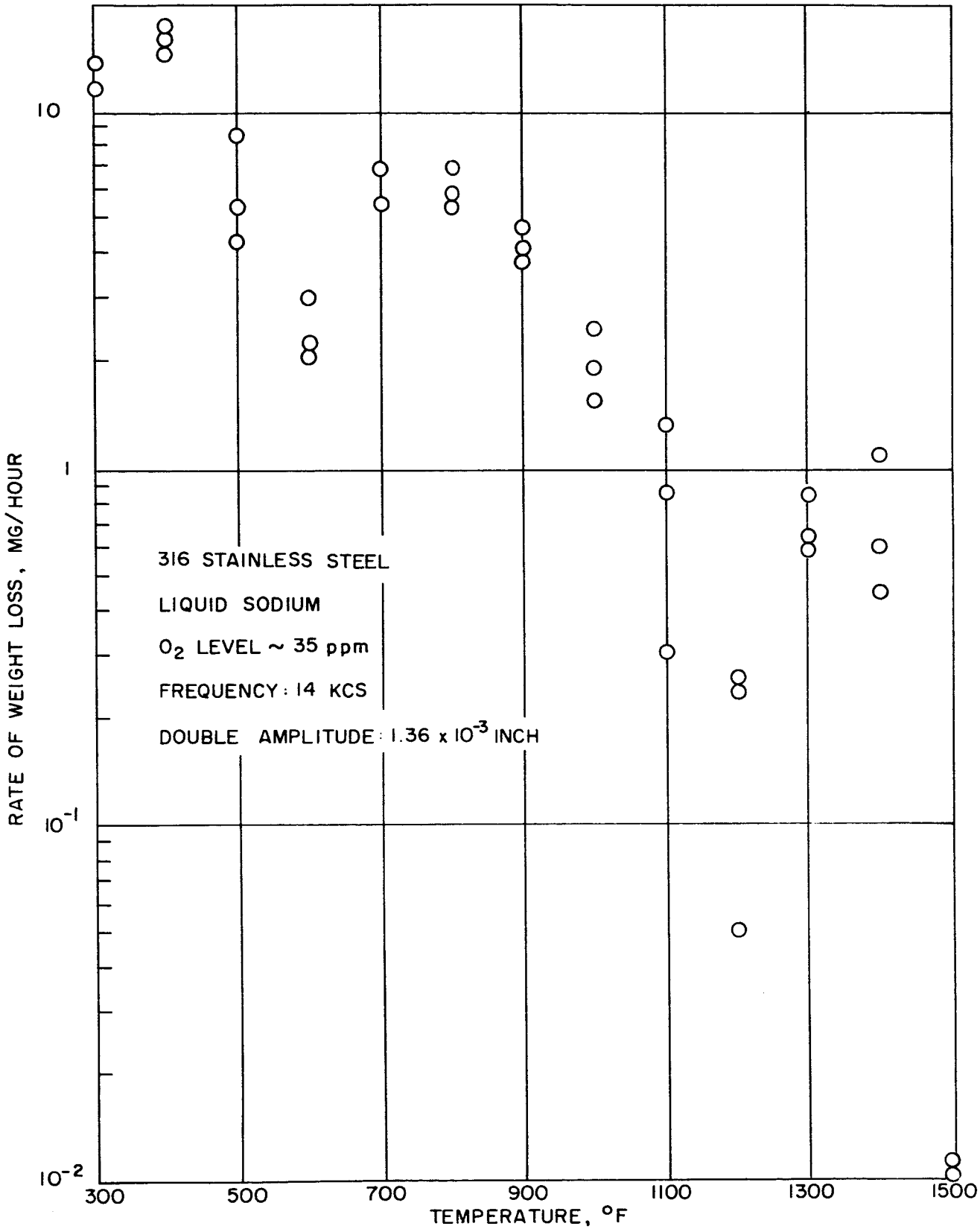

FIGURE 18 - EFFECT OF TEMPERATURE ON THE CAVITATION DAMAGE RATE OF 316 STAINLESS STEEL IN LIQUID SODIUM

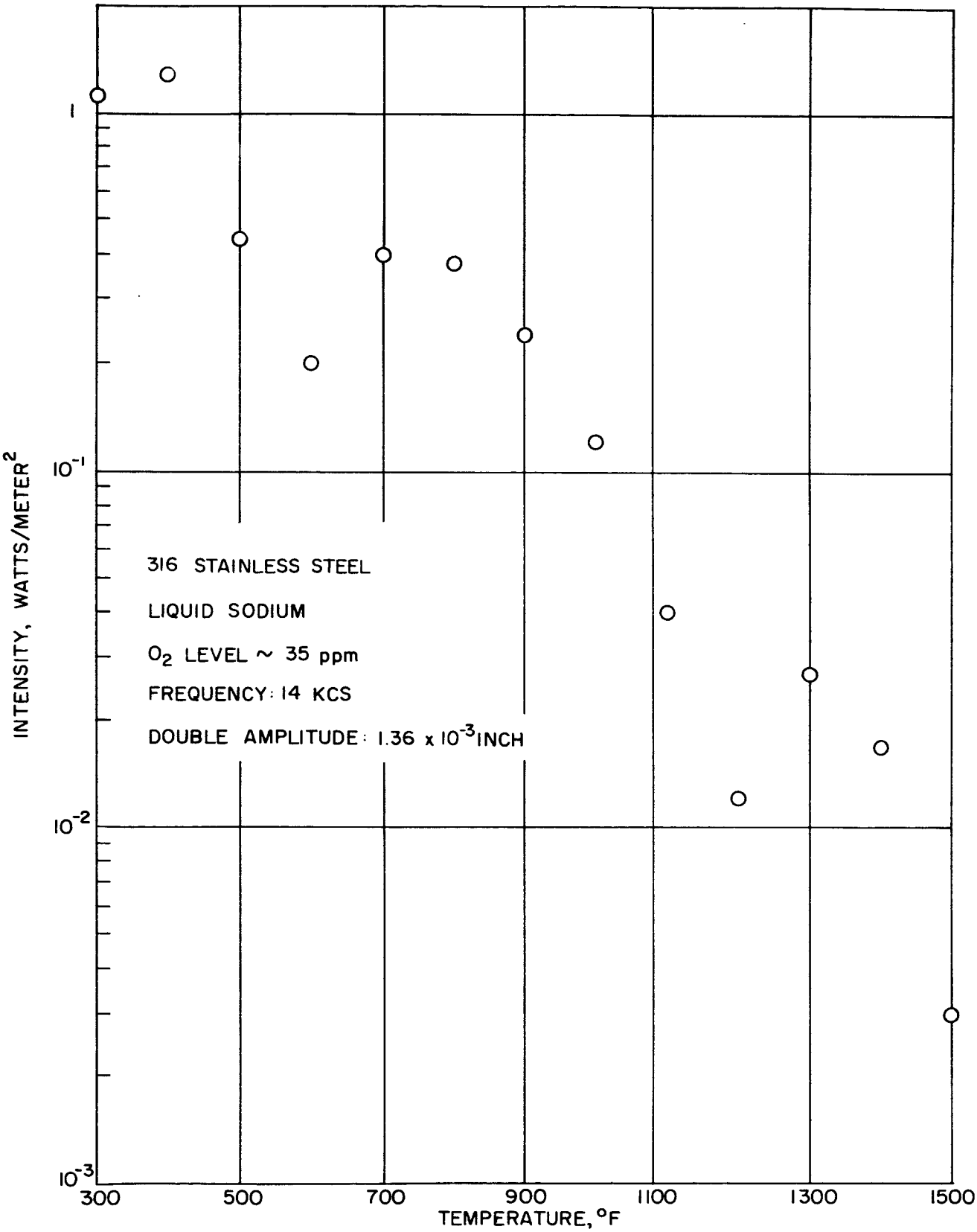

FIGURE 19 - EFFECT OF TEMPERATURE ON THE INTENSITY OF CAVITATION DAMAGE IN LIQUID SODIUM

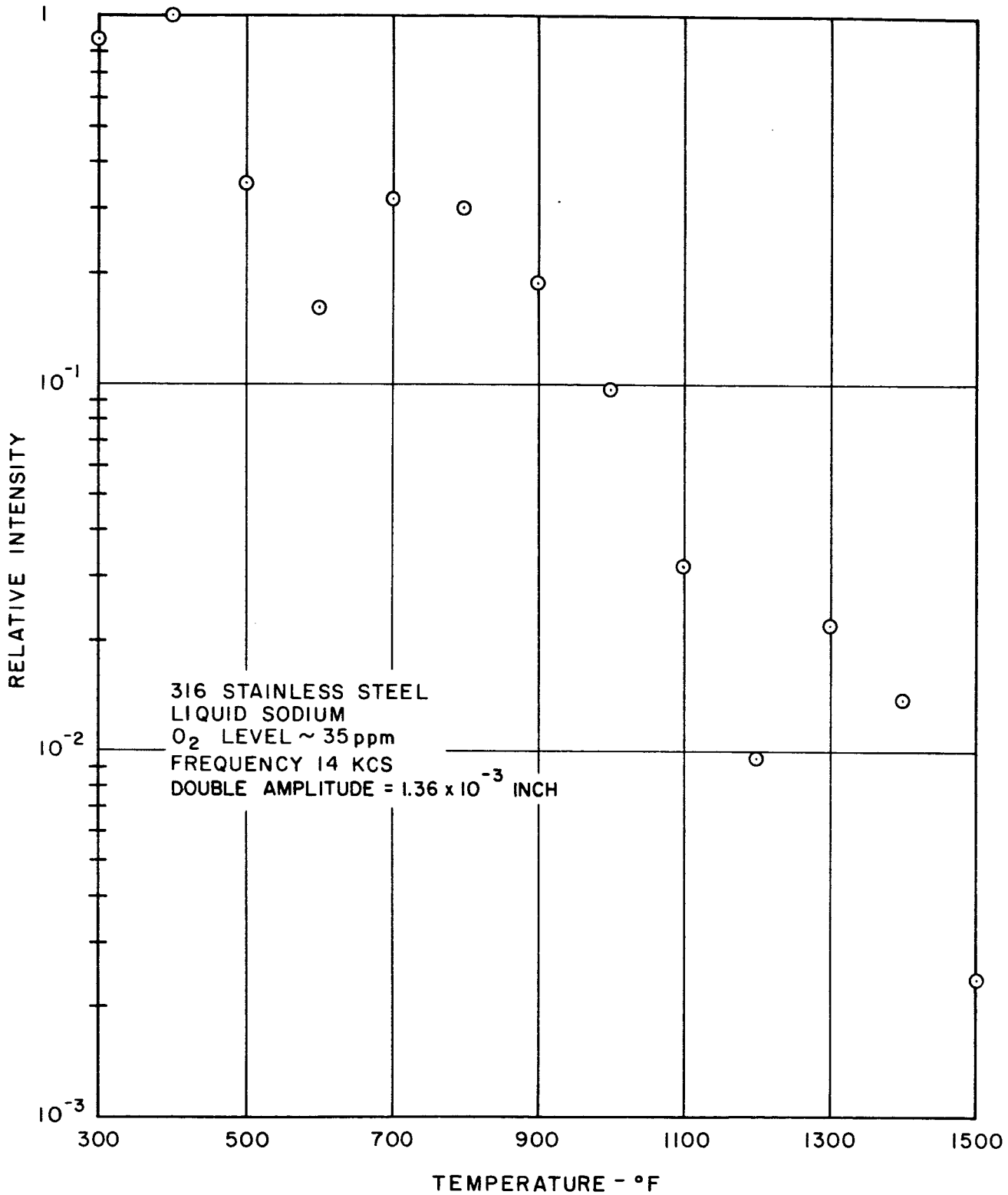

FIGURE 20 - EFFECT OF TEMPERATURE ON THE RELATIVE INTENSITY OF CAVITATION DAMAGE IN LIQUID SODIUM

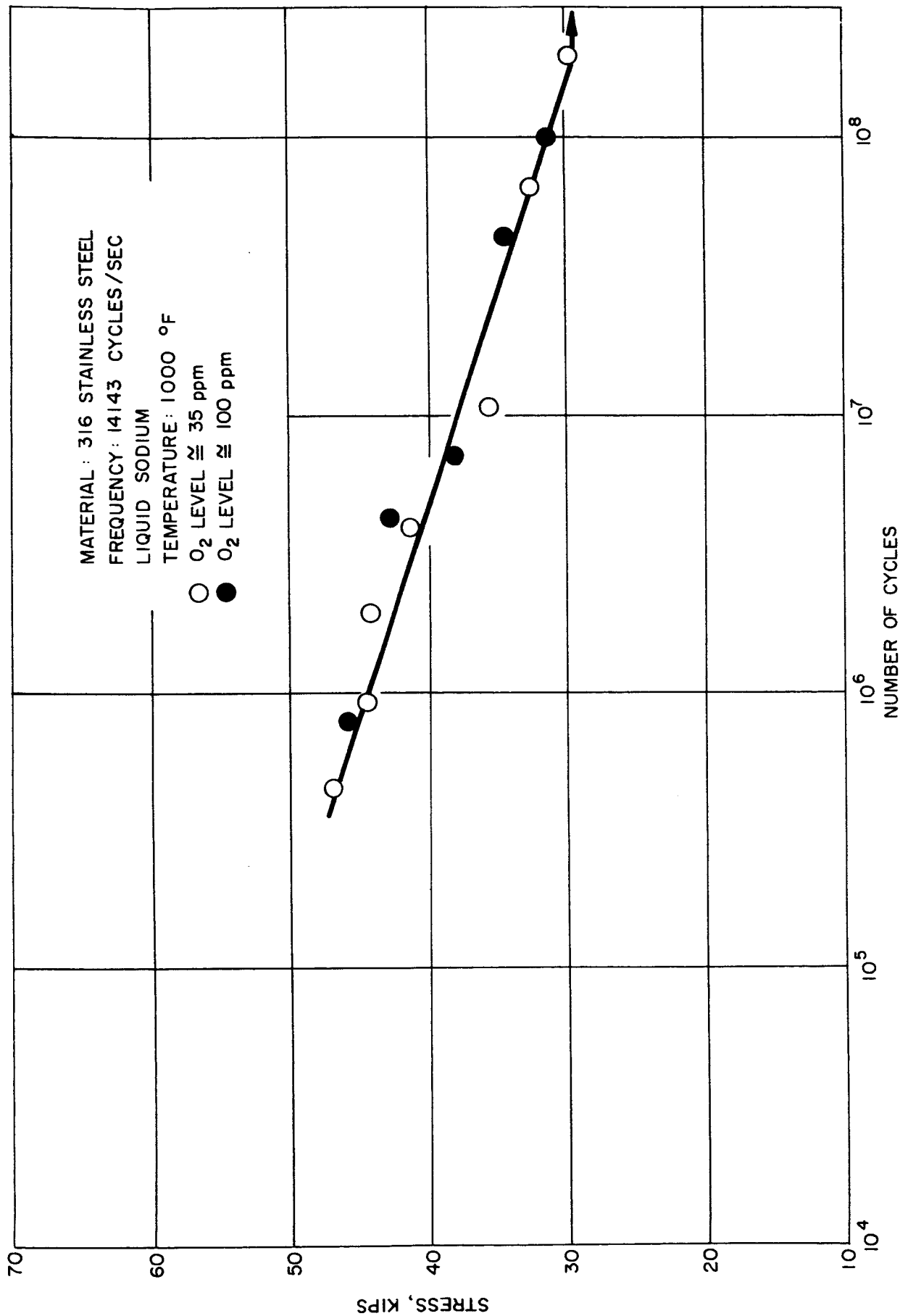

FIGURE 21 - HIGH FREQUENCY FATIGUE OF 316 STAINLESS STEEL IN 1000°F LIQUID SODIUM AT TWO OXIDE LEVELS

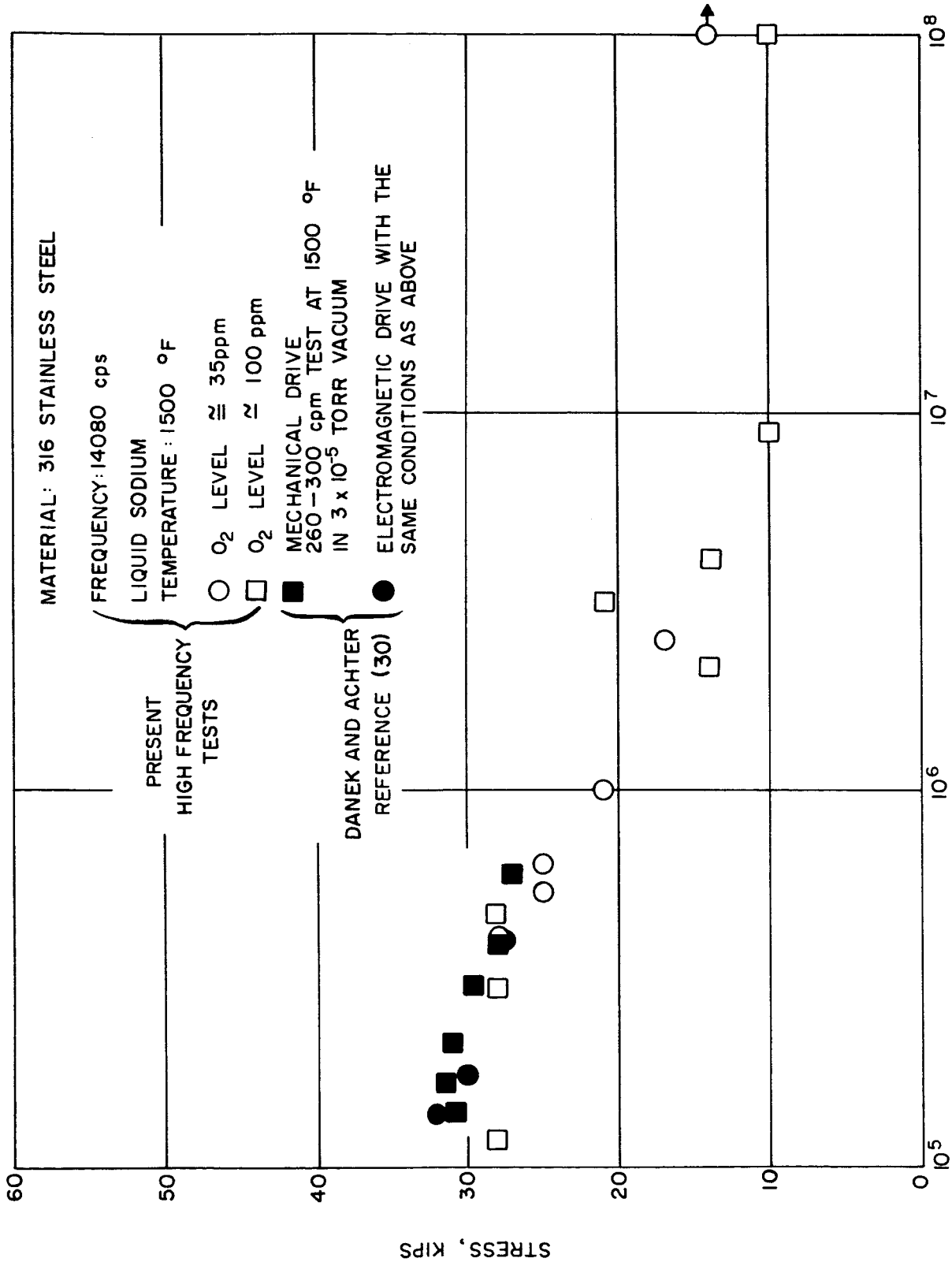

FIGURE 22 - COMPARISON OF HIGH FREQUENCY FATIGUE IN 1500°F SODIUM AND LOW FREQUENCY FATIGUE IN 1500°F VACUUM

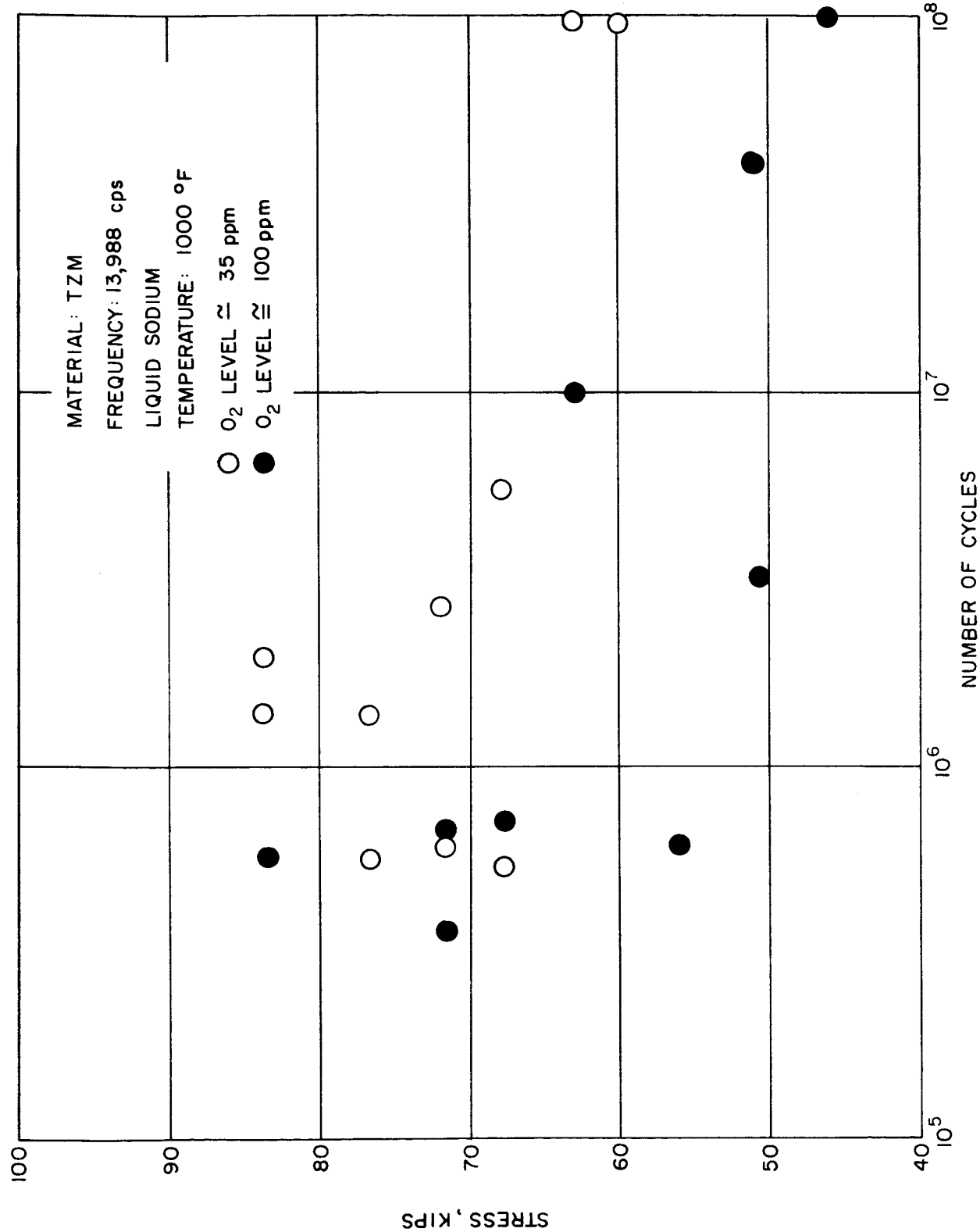

FIGURE 23 - HIGH FREQUENCY FATIGUE OF TZM IN 1000°F LIQUID SODIUM AT TWO OXIDE LEVELS

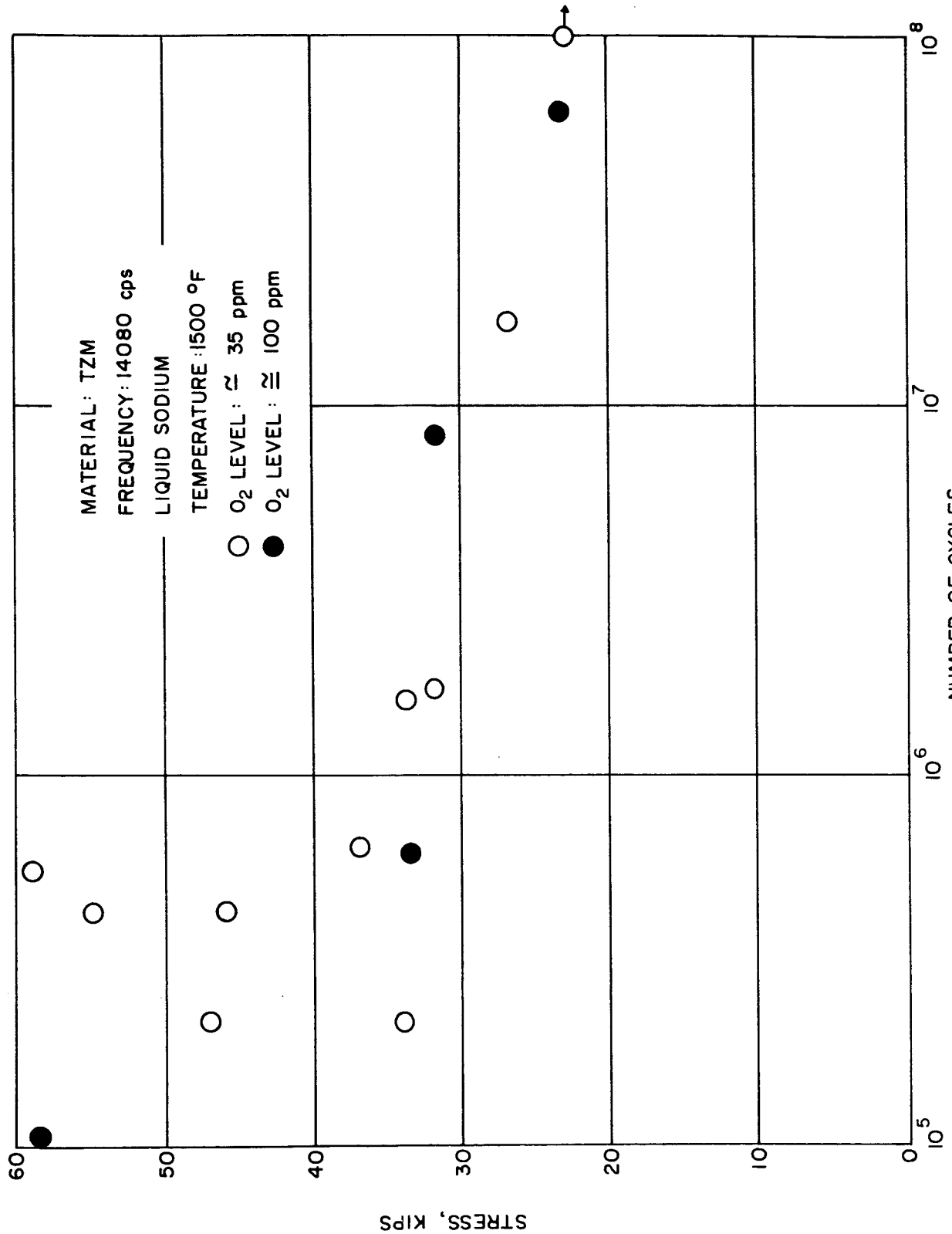

FIGURE 24 - HIGH FREQUENCY FATIGUE OF TZM IN 1500°F LIQUID SODIUM AT TWO OXIDE LEVELS

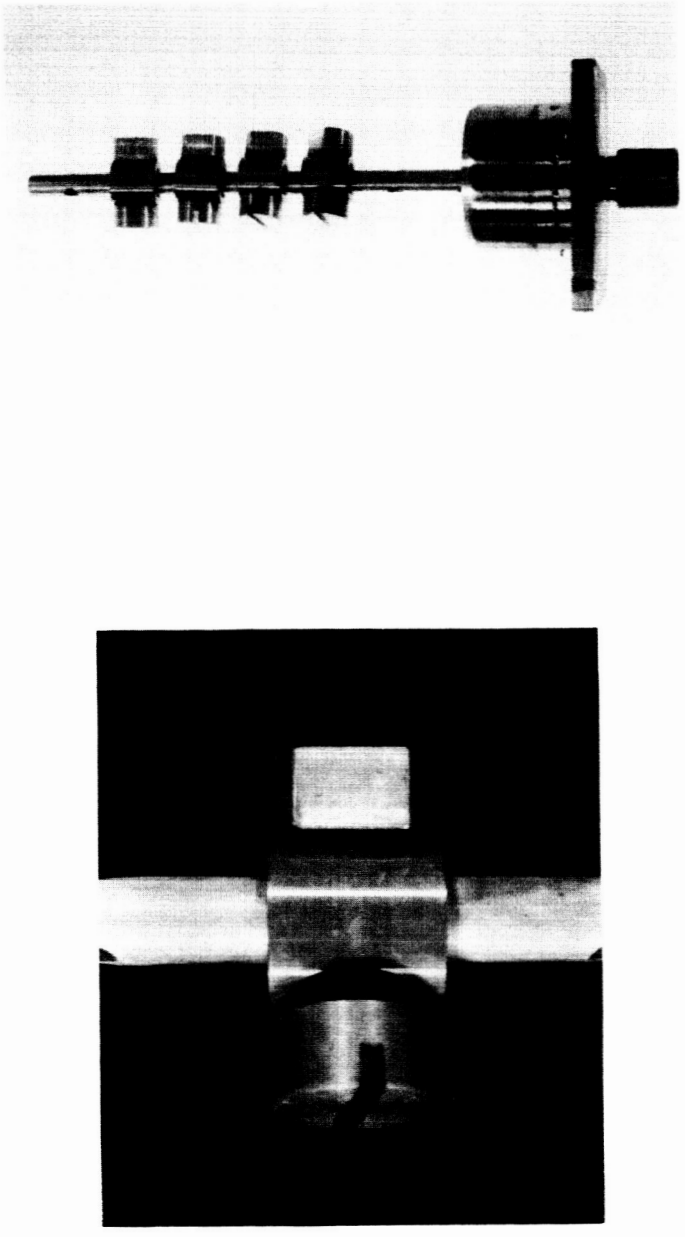

FIGURE 25 - STRESS CORROSION SPECIMENS ASSEMBLED FOR TESTING

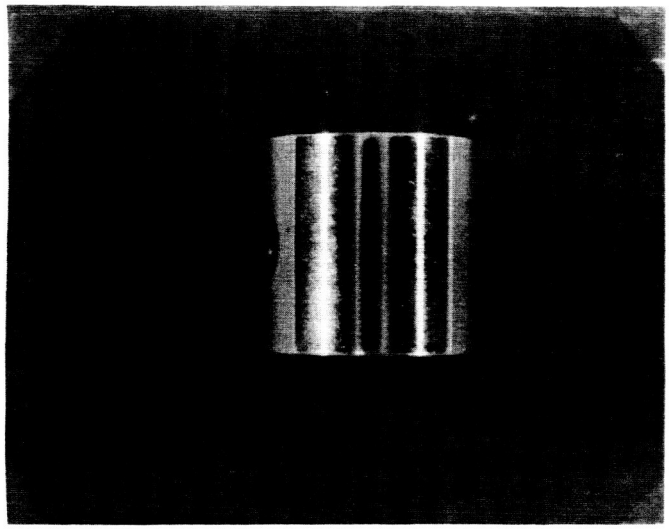

BEFORE EXPOSURE

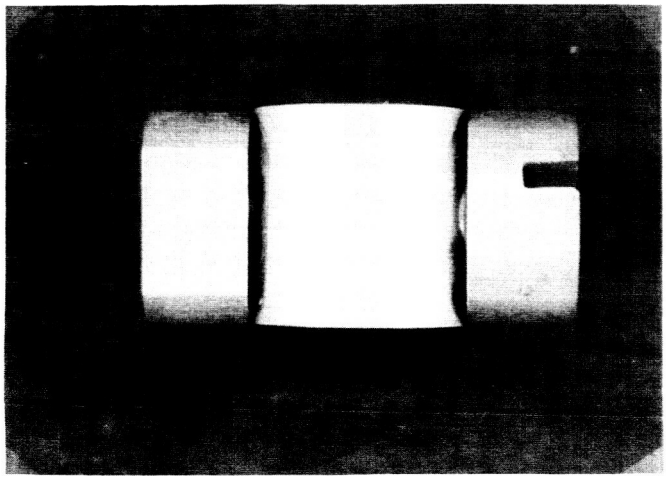

AFTER EXPOSURE

FIGURE 26 - CLOSEUP PHOTO OF 316 STAINLESS STEEL STRESS CORROSION SPECIMEN AT NEAR 100% YIELD AT 1500°F ($O_2 \sim 100$ ppm)

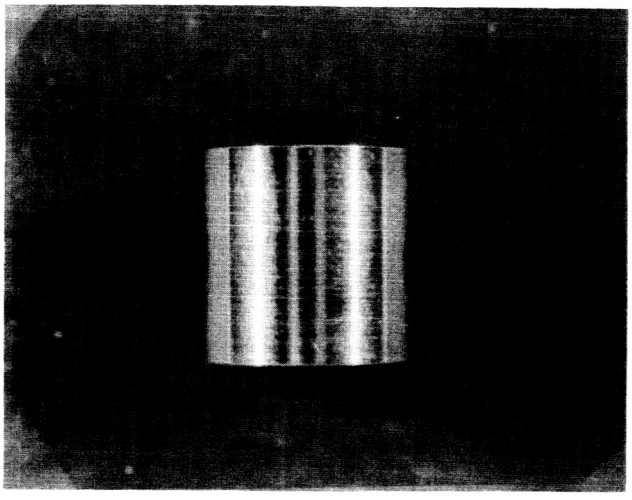

BEFORE EXPOSURE

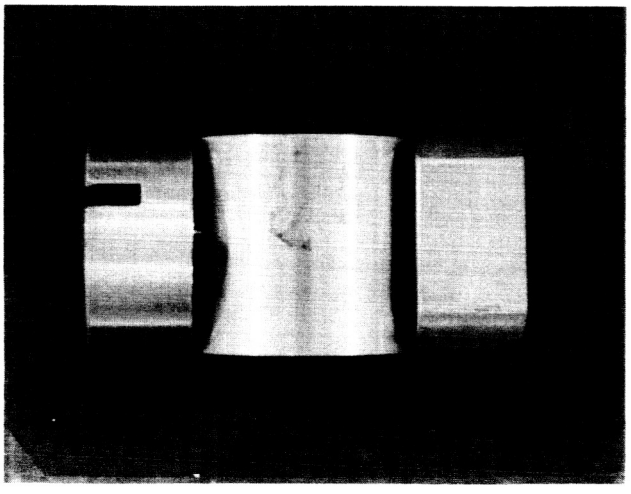

AFTER EXPOSURE

FIGURE 27 - CLOSEUP PHOTO OF TZM STRESS CORROSION SPECIMEN AT NEAR 100% YIELD IN 1500°F SODIUM ($0_2 \sim$ 100 ppm)